February 2002 • NREL/SR-540-31141

Subcontractor Report

Development of a Throttleless Natural Gas Engine

Final Report

John T. Kubesh
Southwest Research Institute
San Antonio, Texas

National Renewable Energy Laboratory

1617 Cole Boulevard
Golden, Colorado 80401-3393

NREL is a U.S. Department of Energy Laboratory
Operated by Midwest Research Institute • Battelle • Bechtel

Contract No. DE-AC36-99-GO10337

February 2002 • NREL/SR-540-31141

Development of a Throttleless Natural Gas Engine

Final Report

John T. Kubesh
Southwest Research Institute
San Antonio, Texas

NREL Technical Monitor: Mike Frailey

Prepared under Subcontract No. ZCI-9-29065-01

National Renewable Energy Laboratory

1617 Cole Boulevard
Golden, Colorado 80401-3393

NREL is a U.S. Department of Energy Laboratory
Operated by Midwest Research Institute • Battelle • Bechtel

Contract No. DE-AC36-99-GO10337

NOTICE

Available electronically at http://www.osti.gov/bridge

Available for a processing fee to U.S. Department of Energy
and its contractors, in paper, from:

U.S. Department of Energy
Office of Scientific and Technical Information
P.O. Box 62
Oak Ridge, TN 37831-0062
phone: 865.576.8401
fax: 865.576.5728
email: reports@adonis.osti.gov

Available for sale to the public, in paper, from:

U.S. Department of Commerce
National Technical Information Service
5285 Port Royal Road
Springfield, VA 22161
phone: 800.553.6847
fax: 703.605.6900
email: orders@ntis.fedworld.gov
online ordering: http://www.ntis.gov/ordering.htm

Printed on paper containing at least 50% wastepaper, including 20% postconsumer waste

Table of Contents

List of Figures

List of Figures Continued

List of Tables

List of Acronyms and Symbols

ϕ	equivalence ratio
BSCO	bake specific carbon Monoxide
BSHC	brake specific hydrocarbons
BSNMHC	brake specific nonmethane hydrocarbons
$BSNO_x$	brake specific nitrogen oxides
BSPM	brake specific particulate matter
BTE	brake thermal efficiency
CAN	controller area network
C_c	craya curtet number
CNG	compressed natural gas
CO	carbon monoxide
COV_{imep}	coefficient of variation of IMEP
DISC	direct injection stratified charge
ECiU	engine control interface unit
EPA	Environmental Protection Agency
FIPC	fuel injected prechamber
FTP	federal test procedure
HC	hydrocarbons
IMEP	indicated mean effective pressure
ISHC	indicated specific hydrocarbons
$ISNO_x$	indicated specific nitrogen oxides
ITE	indicated thermal efficiency
NGP	natural gas pressure (fuel pressure)
NO_x	nitrogen oxides
NREL	National Renewable Energy Laboratory
OC	open chamber
rpm	revolution per minute
SI	spark ignited
SwRI	Southwest Research Institute
VNT	variable nozzle Turbine (variable geometry turbocharger)

Statement of Data Accuracy

The data contained in this report were obtained in a laboratory certified to ISO 9001 standards. An estimate of the data accuracy for relevant parameters is provided below. The accuracy levels shown are based on a percent of full scale unless noted.

Speed: 0.1%
Torque: 1.0%
Pressures: 1.0%
Temperatures: 2.16°F (1.2°C)
Mass Fuel Flow: 0.25% (of reading above 10% of full scale)
Volumetric Air Flow: 0.5%
Emissions: 1.0%

Executive Summary

This report summarizes work conducted under Southwest Research Institute (SwRI) Project 03-2859, "Development of the Next Generation Medium-Duty Natural Gas Engine, Phase II." This project was sponsored by the National Renewable Energy Laboratory (NREL) under Subcontract ZCI-9-29065-01.

The primary focus of the project was to investigate methods to increase the efficiency of natural gas engines, especially under part-load conditions. This report contains details on the development of a natural gas-fueled engine capable of throttleless operation to improve part load efficiency. In-cylinder fuel-air charge stratification was pursued as the mechanism for throttleless operation. Various methods of charge stratification were investigated, including direct injection, stratified charge (DISC) and a fuel injected prechamber (FIPC). The FIPC combustion system was found to be a more practical solution to the problem of charge stratification. Performance and emissions results from this engine configuration are presented and comparisons are made between current natural gas engines and the prototype FIPC engine.

Acknowledgements

This research was sponsored by Stephen Goguen, Program Manager in the Department of Energy's Office of Heavy Vehicle Technologies. The technical monitors for this project were Keith Vertin and Mike Frailey of the National Renewable Energy Laboratory.

The authors would also like to acknowledge several other people who contributed significantly to the project, including Joe Osborne of SwRI, Jason Souder, formerly of SwRI, and Daniel Podnar of Electronic MicroSystems, LLC. Mr. Osborne was the technician responsible for all of the laboratory work, and his contribution was essential towards the successful completion of the project. Mr. Souder was responsible for design and testing of the direct-acting gas injector. Mr. Podnar supplied the control hardware and software required for operating both the direct injection tests and the FIPC engine.

Program Objectives

This program was initiated to investigate the reduction of the part load fuel economy penalty exhibited by current natural gas engines as compared to their diesel engine counterparts. The overall objective of this project was to increase the part load and full load efficiency of a medium duty natural gas engine to that of a state of the art diesel engine. This increase in efficiency was to be obtained while retaining or increasing the emissions benefits provided by current state of the art natural gas engines.

The primary method investigated to reduce part load fuel consumption was to reduce or eliminate throttling losses. Therefore, the specific project objective was to produce a practical throttleless engine, or an engine with significantly reduced throttling losses.

1.0 Introduction

Current natural gas engines tend to suffer from an efficiency penalty compared to the diesel engines they are designed to replace. Figure 1 is a schematic representation of the estimated fuel consumption penalty seen with heavy-duty natural gas engines [1].

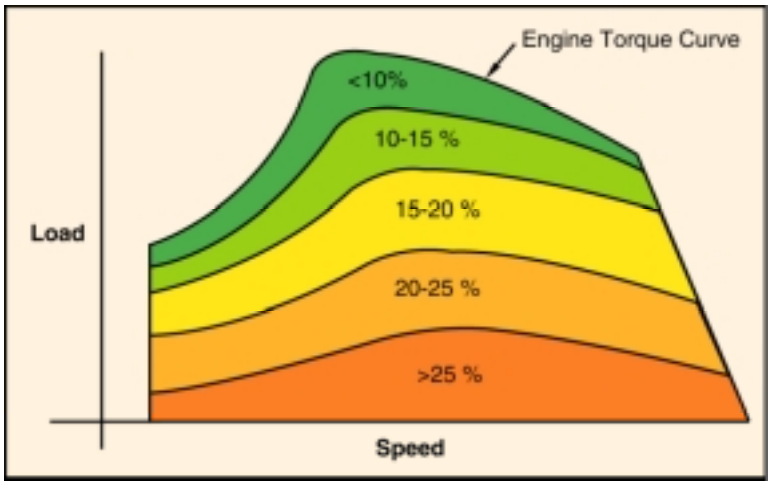

Figure 1. Estimated Fuel Consumption Penalty for Natural Gas Engine versus Diesel Engine (adapted from Ref. 1)

This efficiency penalty is greatest under part load conditions, primarily due to throttling losses. Throttling is required at light loads with engines that use a homogeneous fuel-air mixture. To reduce load, the fuel flow rate must be decreased. However, eventually the mixture becomes so lean that that the lean limit is reached. At the lean limit, combustion of the fuel-air mixture is no longer possible and the engine misfires.

This is illustrated in Figure 2, which shows the fuel-air equivalence ratio required to produce the torque shown at any given speed. These equivalence ratio contours were calculated using an engine model that simulated a naturally aspirated, throttleless engine [2]. As shown, in order to achieve throttleless spark-ignition (SI) operation over the entire engine operating range, the engine must operate at fuel-air equivalence ratios well below the lean limit ($\phi \sim 0.60$) of a homogeneous natural gas-air charge. To achieve these equivalence ratios, the fuel-air charge must be stratified so that an ignitable mixture will be achieved near the spark plug at the time of ignition.

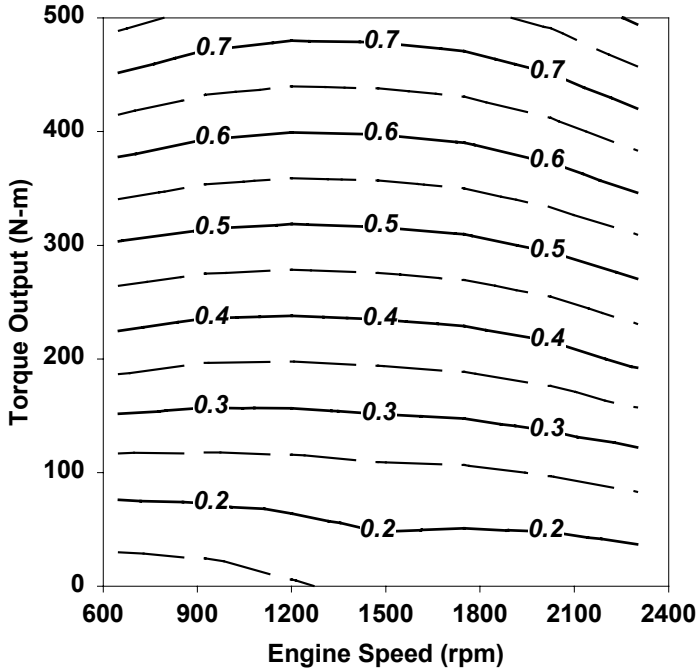

Figure 2. Fuel-Air Equivalence Ratios Required for Throttleless Operation

A variety of stratified charge approaches have been investigated by other researchers with varying degrees of success [3,4,5,6]. Given that a diesel-like diffusion burn approach over the entire operating range was not felt to be desirable for emissions reasons, other approaches were considered for solving this problem, including a prechamber combustion approach, a port injection open chamber combustion approach, and a direct injection open chamber approach. The advantages and disadvantages of each of these approaches were considered. A great deal of work has been done using the prechamber combustion approach with natural gas. Southwest Research Institute (SwRI) has achieved extremely low emissions and high efficiency with prechamber engines operating on natural gas by using very small prechamber volumes, on the order of 2%-3% of the volume of the main chamber [7]. However, in order to achieve throttleless operation over the entire operating range, a much larger prechamber, i.e. approximately 20% or more of the main chamber volume, would be required. SwRI's past experience with engines having prechambers this large has shown that these engines can suffer significant emissions penalties. For this reason, a traditional prechamber approach was originally considered inappropriate for this engine.

Properly timed port fuel injection to achieve charge stratification in an open chamber SI engine has also been attempted [8]. This approach is attractive because it does not force significant modifications to the production engine, i.e. no cylinder head changes would be required and current compressed natural gas (CNG) engines already use port-type gaseous fuel injectors. However, this approach was not likely to provide the level of stratification needed for throttleless operation under very light load conditions.

The initial approach was a direct injection stratified charge (DISC) open chamber SI engine system. Variations of this approach have been successfully developed on light-duty gasoline engines for improving part-load efficiency. The DISC approach was felt to be the best option for allowing throttleless operation, and thus high efficiency, with the lowest emissions penalties relative to a homogeneous charge SI approach. The DISC approach would also facilitate a hybrid stratified charge/homogeneous charge approach to accommodate medium to high load operation.

2.0 Development of Direct Injection Stratified Charge (DISC) System

2.1 Early Direct Injection Engine Development

Note: The work discussed in this section was conducted for an earlier project [2]. This work is included in this report to provide a consistent discussion of the overall project and general background information. Details regarding the project can be found in National Renewable Energy Laboratory technical report NREL/SR-540-27503 [2].

Since no production natural gas direct injectors were available at the beginning of the development project, prototype injectors were developed using readily available automotive technology. The basis of the direct injector design for the project was a fuel metering system developed for a prechamber natural gas engine [9]. This method was adapted for use in a direct injection environment. The fuel injection system used an automotive gaseous fuel injector for the fuel metering element, and a floating ball-type check valve was used to isolate the metering element from combustion pressure and gases. The metering unit also contained the temperature and pressure sensors for calculating fuel density to provide control of fuel mass per injection. Figure 3 shows a solid model of the injector assembly.

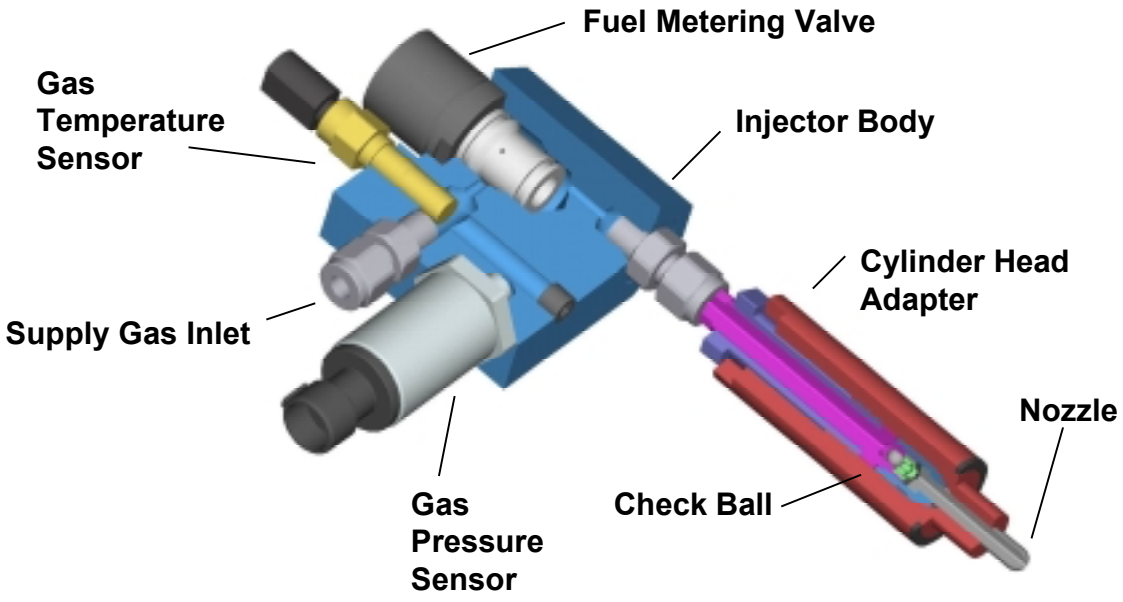

Figure 3. Fuel Injector Assembly

A single cylinder of a John Deere 8.1L CNG engine was converted to the DISC configuration. The intake and exhaust systems for cylinder number six were separated, and the test cylinder was operated as a naturally aspirated engine. The prototype injector was mounted in the normal spark plug location, and the spark plug was relocated to the opposite side of the head through the use of a special adapter sleeve. Figure 4 shows a photograph of the locations of the injector and spark plug in the cylinder head.

Figure 4. DISC Injector and Spark Plug Locations in Cylinder Head
(Left Photograph – Assembled Cylinder Head Right Photograph – Combustion Chamber View)

Initial attempts looked at combustion strategies similar to Texaco engine's spark assisted fuel plume combustion [3]. Multihole nozzles that directed a fuel jet at the spark plug were designed using jet mixing software [2]. Tests proved that these nozzles were not suitable, since they could not provide stable combustion. These nozzles also produced extremely high hydrocarbon (HC) emissions, which indicated that a great deal of fuel was bypassing the combustion process.

Other modern spark-ignited, stratified charge engines, such as the gasoline direct injection engines being developed by companies such as Nissan [10], stratify the charge by injecting fuel into a bowl in the piston that includes the injector and spark plug [11]. These engines are somewhat different because the combustion chamber volume is primarily in the head, compared to the large bowl-in-piston combustion chambers required in natural gas engines derived from heavy-duty diesel engines with vertical valves and a flat fire deck.

The piston was redesigned to incorporate a divided bowl structure. The fuel injector had a nozzle with a large, single hole that vectored the fuel directly down into the primary combustion bowl. In the modified piston design, the piston bowl remained the primary combustion chamber, but the bowl was divided into two sector-shaped regions. One sector of the bowl included the combustion chamber volume directly below the injector tip and the spark plug gap. The other sector constituted the remaining combustion chamber volume. The target compression ratio was increased to 12.0. The bowl geometry was prepared by CNC milling a flat top piston blank. A photograph of the piston is shown in Figure 5.

Figure 5. Prototype DISC Piston

The relative sizes of the combustion bowls were calculated by assuming the primary bowl would contain the amount of fuel required for the engine to produce curb idle torque (~100 N-m) while maintaining a fuel-air equivalence ratio of approximately 0.70 in the bowl and providing a conservative margin from the lean limit.

2.2 Early Direct Injection Results

Tests were conducted with the DISC system to determine the indicated performance and emissions of the test cylinder, and to determine the effects of parameters such as injection timing, spark timing, and injection pressure. The optimum injection pressure was found to be approximately 52 bar (750 psia) and all the test results reported here were obtained at this pressure. The engine operated in a throttleless mode and the overall equivalence ratio values that sustained adequate combustion were well beyond those which could be achieved with a traditional open-chamber lean-burn engine. Equivalence ratios of roughly 0.30 were measured by the emissions bench. This was compelling evidence that the stratified charge combustion strategy was working. Using this system, the load on the test cylinder could be reduced by decreasing the fuel flow to the cylinder. Figure 6 shows how the indicated mean effective pressure (IMEP) of the test cylinder was reduced as the overall airflow ratio was increased (i.e., fuel flow was decreased).

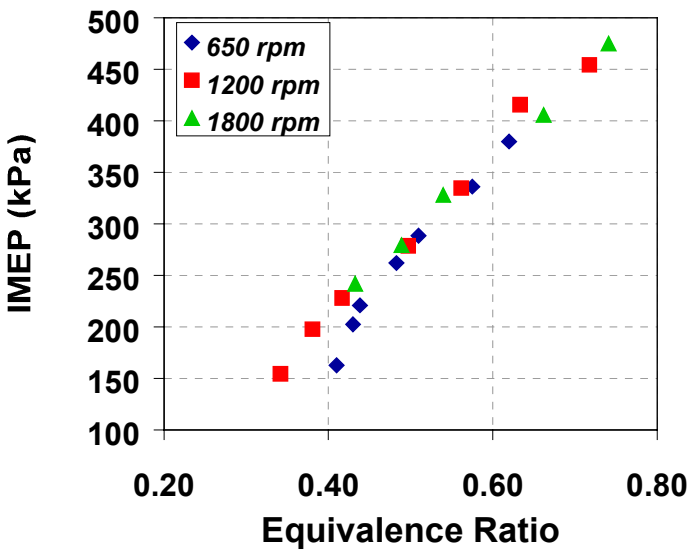

Figure 6. Reduction in Load in DISC Test Cylinder as Function of Equivalence Ratio

Indicated measurements were used to define the load on the cylinder since it was difficult to independently ascertain the brake power output of the single test cylinder. The gross indicated thermal efficiency for these data points ranged from 15% to 30%. These values were reasonable for engines at light loads but were somewhat lower than a comparable homogeneous charge engine. This indicates that the stratified charge combustion process was not as efficient as the homogeneous combustion process. However, since the DISC engine was operating throttleless, little work was lost via pumping and the net indicated efficiency was slightly higher for the stratified charge engine. Assuming the mechanical efficiency of the engine remains constant between the two modes, the brake thermal efficiency of the stratified charge engine would be higher than the homogeneous charge engine. Gains in combustion efficiency would continue to increase and the stratified charge engine's advantage in brake efficiency should continue to increase.

A combustion-phasing problem contributed to the relatively low gross indicated thermal efficiency (ITE) values. Advanced spark timing was found to be required in order to ensure adequate combustion stability. These advanced spark timings caused the combustion event to occur too early in the cycle. Analysis of cylinder pressure data revealed that under most conditions, the combustion process was completed prior to top dead center. A combustion process that releases its energy prior to TDC is inefficient, since some of its energy is wasted in counteracting the upward motion of the piston. Efficiency gains would be realized by shifting the location of the combustion event to after TDC.

The emissions characteristics for the engine were also less than satisfactory. Figure 7 describes the nitrogen oxide ($NO_{x)}$ versus unburned hydrocarbon (HC) tradeoff for the test cylinder for various combinations of control parameters. Both NO_x and HC were quite high compared to a homogeneous charge engine. The high NO_x levels were attributed to combustion regions where the local equivalence ratio was in the range of 0.8-1.0. The high unburned HC emissions were most likely due to fuel gas being swept out of the combustion bowl and into the main piston bowl by the air swirl motion and diluted. Also, fuel trapped in the injector body during compression and combustion was released past the check ball during the exhaust stroke. This was a fundamental limitation of the simple injector design.

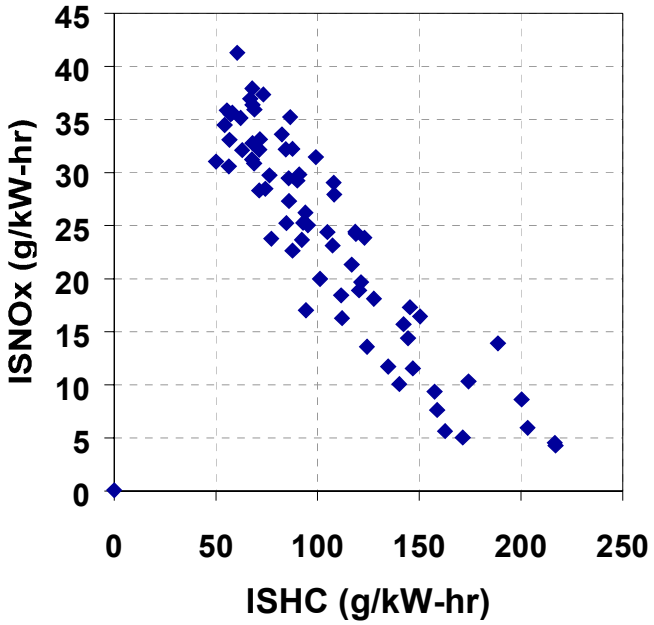

Figure 7. Indicated Specific Hydrocarbons (ISHC) Emissions Tradeoff for DISC Test Cylinder

3.0 Direct Acting Gas Injection System Development

To overcome some of the shortcomings discussed in Section 2, a direct-acting injector was designed and tested. The concept for this type of injector was based on work by Kekedjian and Krepec of Concordia University [12]. Injectors of this type use a combination of a modified diesel nozzle and a commercially available solenoid. A modified Bosch P-type diesel nozzle was obtained from DUAP AG a precision machining company, and a suitable solenoid actuator was purchased from the G.W. Lisk Company. A cutaway view of the prototype injector is shown in Figure 8.

Fuel gas is supplied to the injector through compression fittings located at the top of the injector. The gas flows down through the injector to the diesel nozzle. The gas passes around the solenoid, which should aid in cooling the solenoid during operation. When activated, the solenoid pulls up the needle, thereby admitting gas into the cylinder. At gas supply pressures above 640 psia (~ 44 bar), the flow through the nozzle should be choked throughout the engine cycle. Since the flow will be choked, the mass of fuel injected should be proportional to the injector opening time. A spring is used to return the needle at the end of injection and to keep the nozzle closed against cylinder pressure.

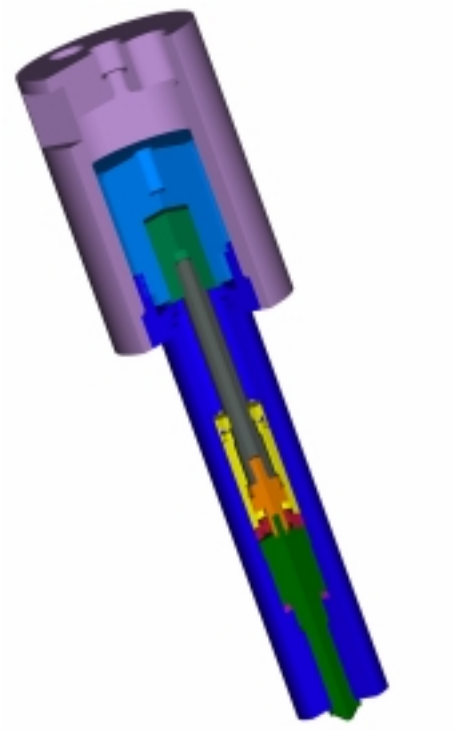

Figure 8. Prototype Direct-Acting Natural Gas Fuel Injector

Bench testing using nitrogen gas was conducted to confirm proper operation of the injector. This testing demonstrated that the injector could meter gas at supply pressures up to approximately 1150 psia (~ 80 bar). Although early testing of the direct injector was successful, problems were encountered with injector needle valve leakage after extended operation due to excessive wear on the needle tip and seat. The wear was traced to the high impact forces on the needle under unlubricated conditions. The high impact forces were caused by the large return spring forces

required to keep the injector needle closed during the compression and combustion processes. When the solenoid was deactivated, the needle assembly was accelerated by the return spring until the needle was seated. The inertia of the large solenoid core and needle assembly was quite high, thereby resulting in high impact forces. Work was conducted to reduce or eliminate these forces. Electric damping of the needle motion using different solenoid closing rates was attempted, and mechanical damping of the solenoid core was also proposed, utilizing a nested spring arrangement that would cushion the needle during seating. Although several of these proposed concepts appeared to be promising for reducing impact forces, no truly practical designs were found.

The main obstacle to reducing the needle seating forces was the requirement for a needle return spring with a relatively high spring constant. The spring was required to provide a strong closing force to counteract compression pressure that acts to open the needle. To overcome this, a poppet valve style injector was designed. Cylinder pressure against the poppet valve acts to keep the valve closed. This type of valve can also be designed to be pressure balanced. Both of these characteristics reduce the amount of spring force necessary. The poppet valve design does have some disadvantages, however. The lack of a single orifice prevents the formation of a well-defined fuel jet and is the primary disadvantage of this application. However, it was felt that a small diameter poppet valve would be capable of directing fuel into a compact piston bowl. The design also requires the use of a “push” type solenoid instead of the current “pull” type.

A prototype poppet valve injector was designed. A cutaway view of the injector assembly for the preliminary design is shown in Figure 9. One concern regarding this injector design was the need for precision grinding on the poppet valve seat required to ensure a leak-proof valve.

Figure 9. Cutaway of Poppet-Valve Direct Gas Injector

Fabricating the poppet valve injector was put on hold due to concern over the practicality of the direct injection concept. The development of the DISC concept encountered many difficulties, such as needle wear, and accurate fuel delivery. Other problems were anticipated, including solenoid durability, overall injector cost, and overall reliability. Due to these concerns, other strategies for producing a throttleless gas engine were investigated. Designs that used divided combustion chambers to provide mechanical stratification of the fuel-air mixture appeared to be more practical than direct injection technologies that require the formation of a stratified mixture within a changing geometry. This led to the development of the Fuel Injected Prechamber (FIPC) engine concept.

4.0 Development of Fuel Injected Prechamber (FIPC) System

The divided chamber engine underwent a great deal of research until the late 1970's, at which time emissions requirements precluded their use in favor of engines utilizing three-way catalysts and exhaust gas recirculation. Prior to this, various researchers had developed these engines to practical levels [13, 14]. These divided chamber gasoline engines were successfully operated without throttling at part load with reasonable emissions levels. The concept was also similar to that developed by Ritter and Wood [15] for a throttleless natural gas conversion of a two-stroke diesel engine. SwRI also had experience in designing prechambers for large engines. These prechambers are usually small in size and are used as an ignition assist for very lean mixtures and to increase the combustion rate of large bore engines. Based on input from the stratified charge literature and practical design experience, a divided chamber combustion system was designed.

The operational strategy for this combustion system was to operate the engine at part loads by fueling the prechamber alone and modulating torque by adding fuel (termed "fuel mode"); this strategy is similar to that of a naturally-aspirated diesel engine. At higher loads, fuel would be added to the main chamber to form a homogeneous charge and the prechamber would act as the ignition source, in a manner similar to a conventional prechamber gas engine. Load would be controlled by air flow to the engine (or "air mode"). Air flow would be modulated using a variable geometry turbocharger.

A cutaway of the initial divided chamber design is shown in Figure 10. The prechamber was located in the current spark plug hole location, with the spark plug cavity forming the prechamber chamber. The prechamber nozzle was mounted in the modified spark plug hole. An automotive natural gas fuel injector that was isolated from the prechamber by a ball-type check valve fueled the prechamber. Figure 11 is side view of the prechamber assembly as installed in the head.

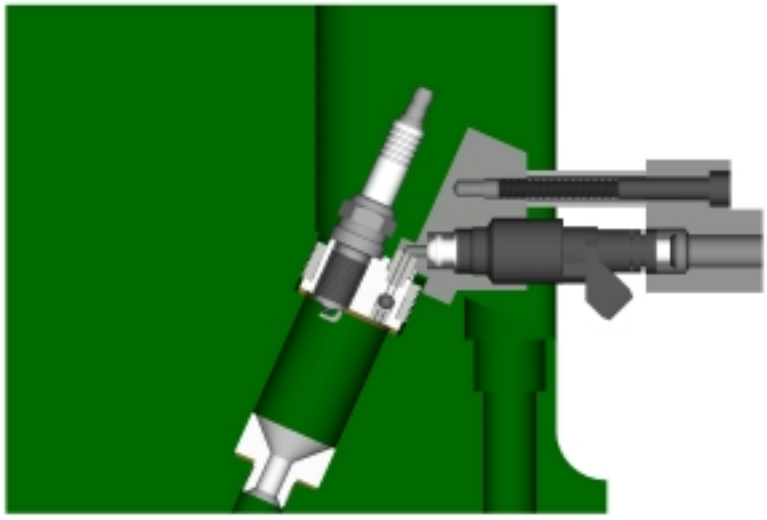

Figure 10. Cutaway of Prechamber Design

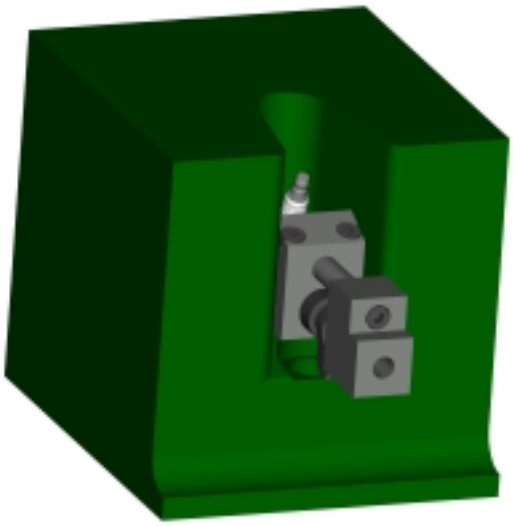

Figure 11. Side View of Cylinder Head and Fuel Injector Mounting Block

SwRI prechamber design software was used to calculate the appropriate prechamber dimensions. A prechamber volume equal to 20% of the total combustion chamber clearance volume was chosen for the initial design efforts. This volume was large enough to contain sufficient fuel-air mixture to operate the engine at light loads over the speed range of the engine. Gruden [13] also indicated that the prechamber volume should be 20% or less for good results in terms of emissions and fuel economy.

Table 1. Prechamber Specifications

Prechamber Parameter	Dimension
Volume	20% of clearance volume
Nozzle diameter	7.25 mm
Craya-Curtet Number	0.291

The Craya-Curtet (C_c) number shown in the table is a non-dimensional number that describes the level of mixing that takes place inside the prechamber while filling during the compression stroke. It has been shown that C_c has an important effect on the performance of the prechamber [16]. As a general rule, a prechamber with a C_c less than 0.3 will provide good performance in a natural gas engine. In addition, the ratio of the nozzle orifice area to the prechamber volume was approximately 0.02. This value corresponded well to the range of ratios that gave good performance on the Porsche SKS engine [13].

The engine was subsequently converted to the FIPC configuration. All six cylinders were modified since we were confidant that that the FIPC system could be developed without the need for single cylinder testing. The cylinder head was machined to accommodate the prechamber caps, nozzles, and fuel injector blocks. The engine fuel system and control system were modified as required. A fuel rail to feed the prechamber injectors was fabricated, and a production fuel metering block was adapted to provide pressure and temperature compensation as well as fuel shut off capability. Fueling for the main chambers was provided by a proportional metering valve with fuel introduction through the production fuel-air mixer. The throttle was retained on the

engine but was held at the 100% open position for all testing with this configuration. Figure 12 is a schematic of the fuel system showing the various components, and Figure 13 is a photograph of the fuel system as installed on the engine.

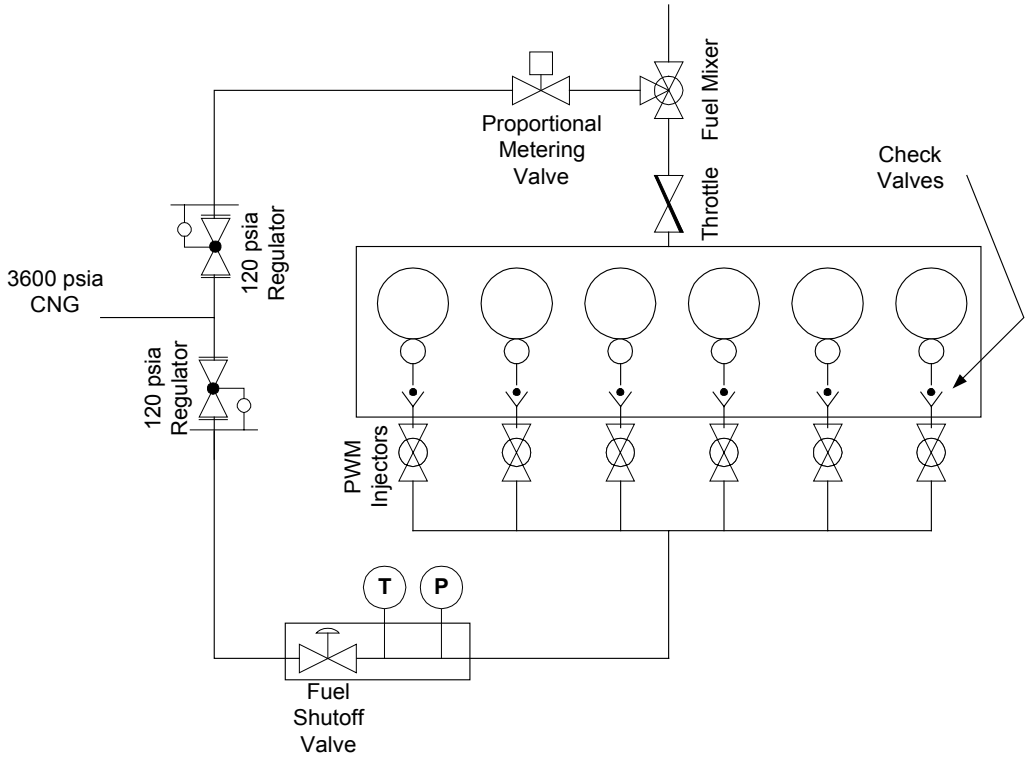

Figure 12. Schematic of Original Prechamber Fuel Metering System

Figure 13. Prototype Fuel System with Initial Design for Direct Prechamber Fueling

The piston was also modified. The piston bowl was reduced in volume to compensate for the additional volume in the prechamber so that a compression ratio of 11.3:1 was obtained. This compression ratio was the same as used for a low emissions gas engine developed under a previous development program [17]. The piston had the simple geometry shown in Figure 14. The bowl was offset from the centerline of the piston so that the centerline of the prechamber jet would intersect with the center of the piston bowl at TDC. Since the piston position stays relatively constant near TDC, this was considered the best compromise on bowl location. The effective squish area was increased to 57%, higher than most typical natural gas engines, and this was expected to increase the burn rates of lean mixtures. After conversion, measurements showed the PC volume to be approximately 19% of the clearance volume. This was within 5% of the target volume fraction of 20%.

Figure 14. Piston Design Used for Divided Chamber Engine Experiments

Engine control was provided by an engine control interface unit (EciU) prototyping engine controller obtained from Electronic MicroSystems. This "production-like" prototyping controller is based on the Infineon C167 microcontroller used in the production Deere diesel engine control system, and was similar to those used on other Deere development projects at SwRI. The system also had more capacity and was more flexible than the PC/DOS-based system used previously. The ECiU is a hybrid system; i.e. it uses a microcontroller to interface with the engine's sensors and actuators in conjunction with a PC for performing the necessary control calculations. The two computers communicate via a high speed Controller Area Network (CAN) link. The PC provides a flexible platform for control software development, and the microcontroller provides a robust interface with the engine and enables the use of the production wiring harness and sensor package with minimal modifications. A photograph of the completed controller as installed on the engine is shown in Figure 15. Since the new controller utilized the production wiring harness for most of the interfacing to the engine and only minimal additional wiring was necessary for the direct injection engine, the complexity of the wiring between the cell interface computer and the engine controller unit was reduced considerably.

The ECiU was configured to operate the six prechamber injectors independently along with the proportional metering valve, and the control software was reworked for the new dual mode control scheme. One of the control modes was the air control mode. This mode is the same as that used in typical gas engines, where load is controlled by modulating the air flow to the engine with a throttle. In this mode, the engine could be operated on main chamber fueling along or with some percentage of fuel metered through the prechamber. The other mode was the fuel control

mode, used for operating on the prechambers alone. This mode used the throttle command (or pedal input) as a torque command, similar to a diesel engine. In this mode, as the requested torque was increased, the fuel metered to the prechambers was increased accordingly. This mode was designed to allow the engine to run at light loads on the prechambers.

Figure 15. ECiU Prototyping Engine Controller

During initial testing, the engine was started and operated satisfactorily in the air control mode. The engine ran rougher than the production engine, probably because the prechambers are trapping residual gas near the spark plug, and the spark plug is exposed to an overly dilute charge on some cycles. In the air control mode, no fuel was supplied to the prechambers; the prechamber was designed to be scavenged by the prechamber fuel, so this lack of scavenging may have caused the rougher operation.

Problems were encountered when attempting to run the engine on the prechambers alone or with substantial prechamber fuel rates. In fact, the engine only ran on the prechambers alone for a short time. Following these attempts, the engine would not start and run at all on the prechambers alone nor would the engine run on the prechambers alone after any extended running in the air control mode.

During attempts to run on the prechambers alone, it was noted that the exhaust equivalence ratio was near zero. This indicated that no fuel was reaching the prechambers. An injector indicator light plugged into the wiring harness showed that the injectors were receiving a firing signal. An oscilloscope was then used to verify that the prechamber injectors were being fired at the correct time during the cycle and the injectors and cylinders were matched correctly. This troubleshooting eliminated the controller as the source of the problem, and the prechamber fuel system was suspected.

Observations of the regulated natural gas injector supply pressure (NGP) revealed that the NGP began steadily increasing as the engine was run, until the NGP sensor reached its maximum value. From this, it was surmised that the prechamber check balls were leaking. This would allow the cylinder gases to push open the injector momentarily and fill the space between the injector and the CNG regulator. After several cycles, the line pressure would then be raised above the regulator setpoint and the regulator would clamp off the line, since the regulator is a non-relieving type. After each cycle, more gas would be trapped in the line, thereby increasing the pressure steadily. At some point, the injectors could not open since the line pressure was above the injectors' maximum opening pressure, so any attempt to run on the prechamber fuel system alone would fail.

To verify that the check balls were leaking, the prechamber injector assemblies were removed and the engine was operated on main chamber fueling alone in the air control mode. At low speeds, the engine rattled noticeably, but a surprisingly small amount of flow was found coming from each cylinder. Under some conditions at higher engine speeds, the engine quieted down and almost no flow could be detected coming from the check valve holes. This experiment showed that some reverse flow through the check valves could be expected and provisions for handling this flow were necessary.

The solution to the trapped gas problem was to increase the volume between the check valve and the injector. To counteract the pressurization effect, the injectors were relocated to a central location and connected to the prechamber through a length of tubing. The increased volume of the line prevented the excessive rise in pressure at the injector exit. A schematic of this configuration is shown in Figure 16.

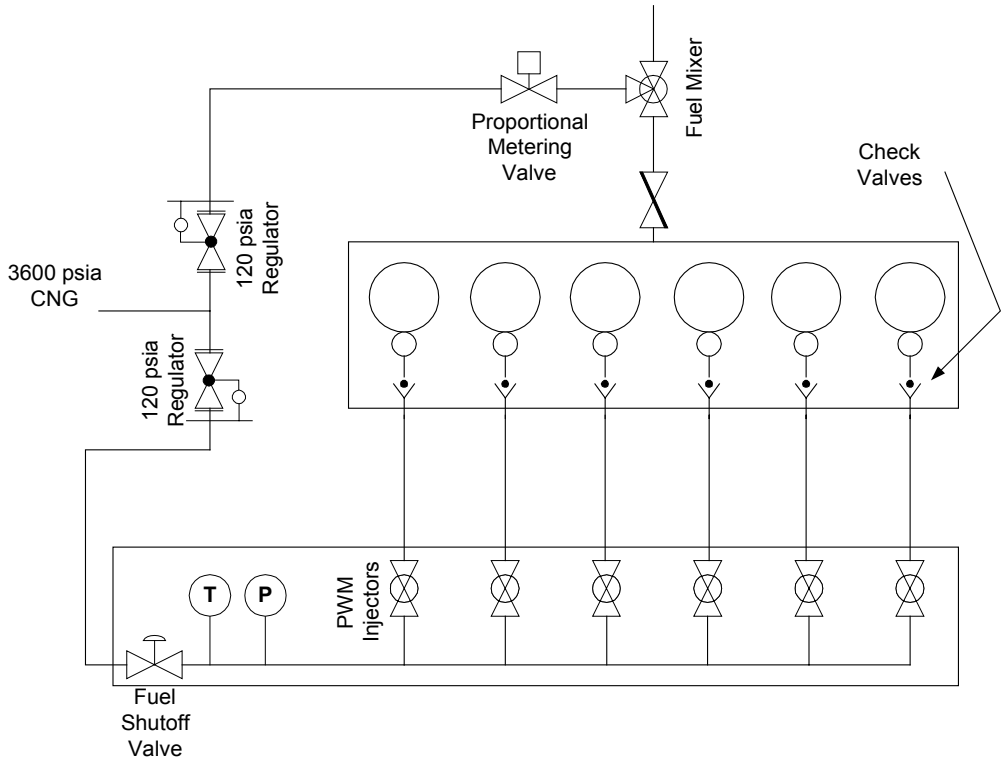

Figure 16. Schematic of Revised Fuel Metering System with Increased Volume between Prechamber Fuel Injectors and Prechamber Check Valves

A short period of testing was then conducted to verify that the engine was functioning correctly. The base engine ran well, but some irregularities were noted with the prechamber fuel system. During operation, it was noticed that the fuel injectors would periodically "jump" in their mountings. It was surmised that this motion was caused by a combustion pressure pulse that was able to propagate past a prechamber check ball that did not seat completely on that cycle. To eliminate any possible damage to the injectors, a secondary set of low pressure drop check valves were installed between the prechamber check valve and the fuel injectors as additional protection. Figure 17 is a schematic of the modified fuel system configuration and the photograph in Figure 18 shows the engine in this configuration. Independent fueling of each prechamber was accomplished.

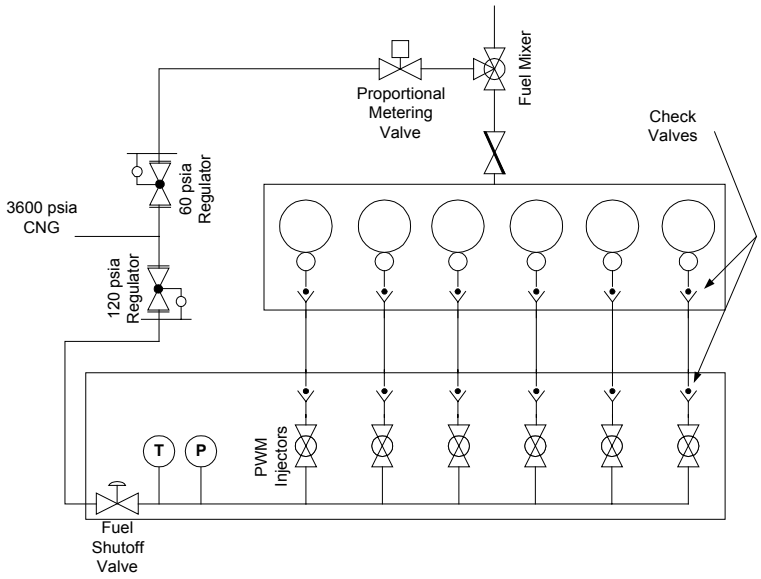

Figure 17. Schematic of Fuel Injection System

Figure 18. Photograph of FIPC Engine with Final Configuration Prechambers and Fueling System

Subsequent testing at high loads illuminated another problem with the prechamber fuel system. The prechamber cap cooling was found to be insufficient for the high heat flux at high loads. Due to the high temperatures encountered, the o-ring seal in the connection between the original prechamber injector mounting block and the prechamber cap would deteriorate over time and begin to leak. High temperature Viton o-rings were tried as a stopgap measure, but this succeeded only in lengthening the time between failures. Also, the temperature cycling between high and low loads caused the prechamber hold-down nut to loosen over time. A new, more reliable method was therefore needed to provide both the fuel delivery to the prechamber as well as to provide a more robust way to hold down the prechamber cap.

The fuel system was modified to eliminate the o-ring connection. The injector blocks were removed, and direct fuel tubes were silver soldered into place. New prechamber cap hold-downs were machined to provide clearance for the fuel tube and spark plug. These new cap hold-downs were designed to provide all of the hold-down force, but prechamber hold-down nuts were also installed for secondary protection. Figure 19 is a photograph of the revised fuel system components, including the new fuel tube and prechamber cap hold-down.

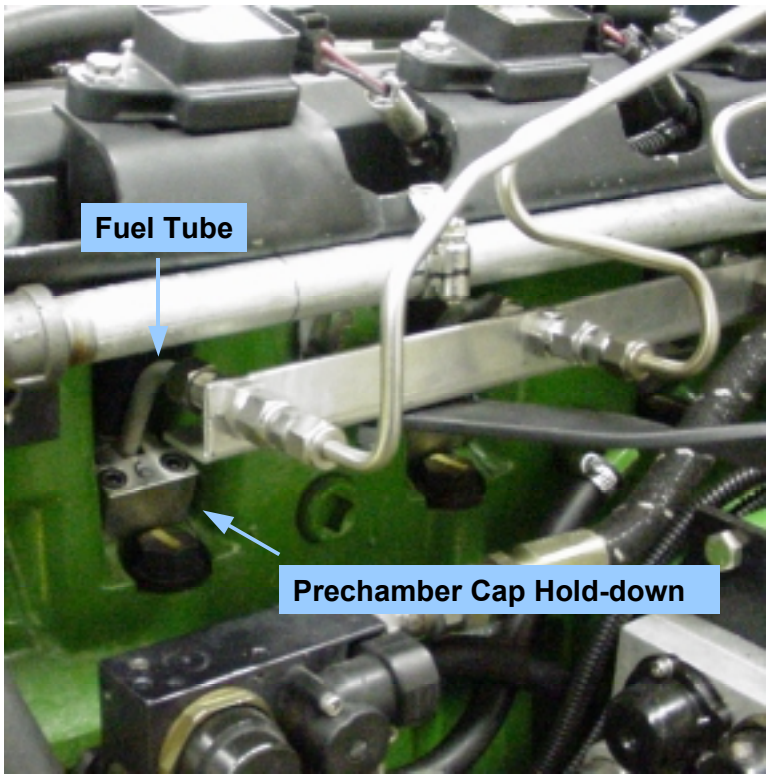

Figure 19. Photograph of Improved Fuel Delivery Tube and Prechamber Cap Hold-Down

An apparatus for cooling the spark plugs and top of the prechamber was also installed in response to a spark plug failure on the engine. During high load testing, the center electrode of the spark plug on the rearmost cylinder became detached from the body of the spark plug and was ejected by combustion pressure. The cause of the failure may have been excessive thermal growth of the spark plug body or simply a defective spark plug. In either case, it was prudent to devise some way to cool the spark plugs. The method chosen was to install an air cooling tube. This tube had a

series of six small holes that pointed at one side of each spark plug. The air jet supplied by this hole flows around spark plug body to cool it. The concave shape of the spark plug cavity in the head redirects the flow around the spark plug, thereby carrying the heat away from the engine and cooling the spark plug. A photograph of the cooling tube is shown in Figure 20.

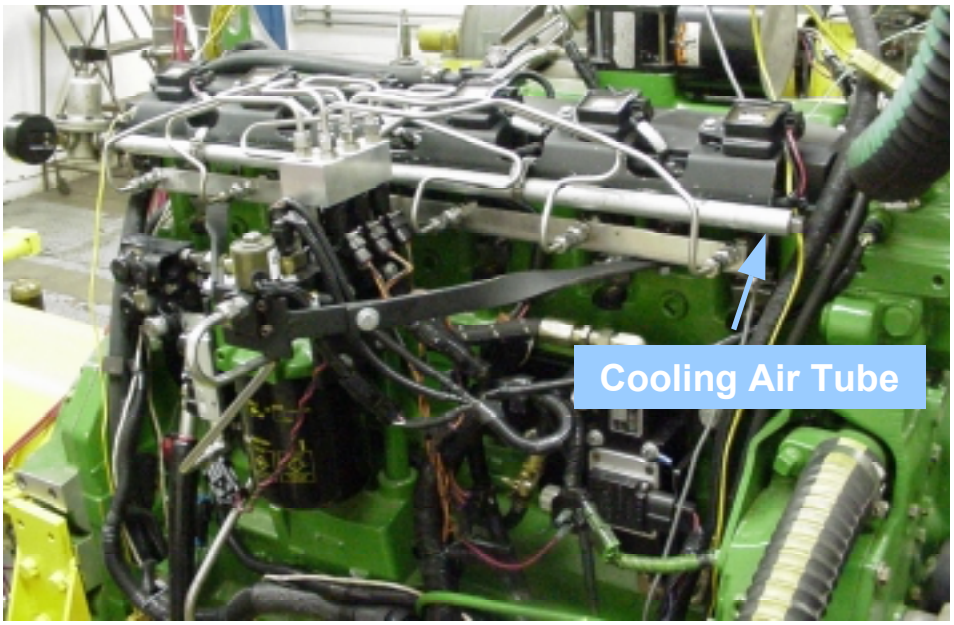

Figure 20. Photograph of Cooling Air Spray Tube Mounted on Engine

Changes were also made to the turbocharging system. To this point, the torque output of the divided chamber engine had been controlled either by the fuel flow rate (fuel control mode) or by the air flow rate (air control mode). In air control mode, the air flow rate was varied using the turbocharger wastegate to control boost pressure. Previous results [2] showed that a variable geometry turbocharger could be used to adjust load on a typical natural gas engine. The engine and the control system were modified to accommodate a Garrett VNT40 variable nozzle turbine (VNT) turbocharger. Figure 21 shows the VNT40 as installed on the engine, along with the modified control equipment used for actuation of the variable nozzle mechanism. A natural gas fuel injector was used to supply air to the pneumatic actuator; control was accomplished through pulse width modulation of the injector and a small bleed orifice on the actuator. Preliminary operation of the engine under steady state conditions confirmed that the VNT40 could produce sufficient air supply for very lean operation over the speed and load range required.

Figure 21. Photograph of Variable Geometry Turbocharger Installation

5.0 Results with FIPC Engine

The engine and fuel system worked well with this configuration. Extensive engine testing was conducted to determine the optimum combination of overall equivalence ratio, spark timing, prechamber fuel fraction, and prechamber injection timing. The resulting calibration produced the torque curve shown in Figure 22.

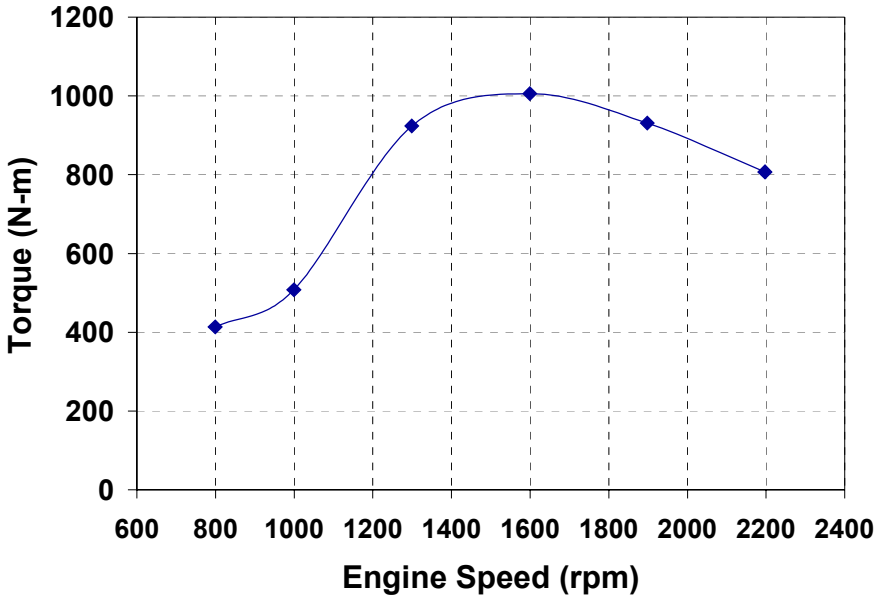

Figure 22. Torque Curve for FIPC Engine

Performance and emissions measurements were subsequently measured over the wide speed and load range. The engine was operated with the throttle at the full open position for all points. Under all conditions, the engine performed well and was capable of throttleless operation. Light loads were obtained by reducing the equivalence ratio below that of the typical lean misfire limit for natural gas engines. Since ignition takes place in the rich prechamber, and the very lean main chamber is ignited by the very energetic prechamber jet, the overall equivalence ratio was much lower than that which could be attained with an open chamber spark-ignited engine. Figure 23 is a plot of the equivalence ratio (ϕ) calculated from the exhaust gas measurements. Note that for torque levels below roughly 400 lb-ft, the engine operated at an equivalence ratio below that normally seen as the leanest operating point for an open chamber engine, e.g. $\phi \approx 0.60$. Although not shown in the mapping data presented in Figure 4, additional tests confirmed that the engine could operate in a throttleless mode down to the minimum load level required to maintain a constant speed, with $\phi < 0.30$.

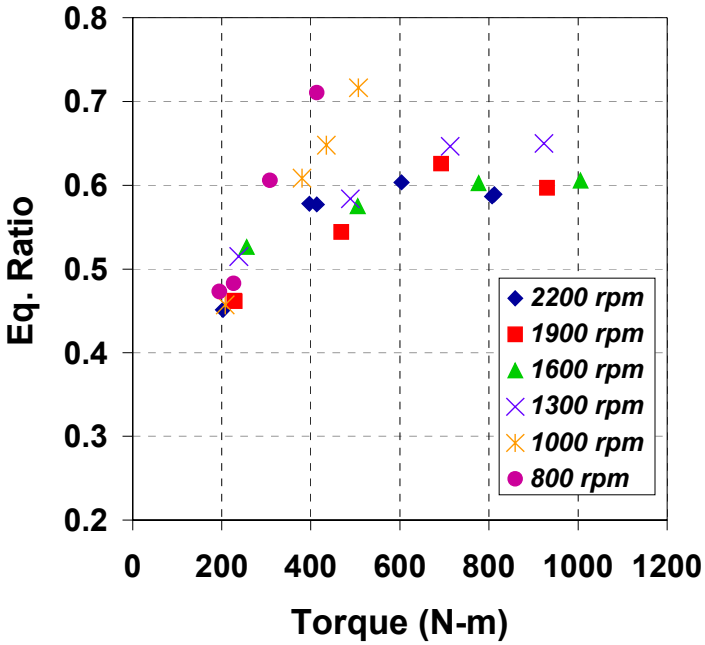

Figure 23. Fuel-Air Equivalence Ratio for FIPC Operation

Thermal efficiency results for the engine are shown in Figure 24. The results are fairly good, especially considering that the data represents the initial attempt at operating this combustion system above low load levels. The full load efficiency ranged from 32.8% to 36.3%. However, even when using the optimum combination of parameters, the engine did not provide an improvement in efficiency compared to existing engines.

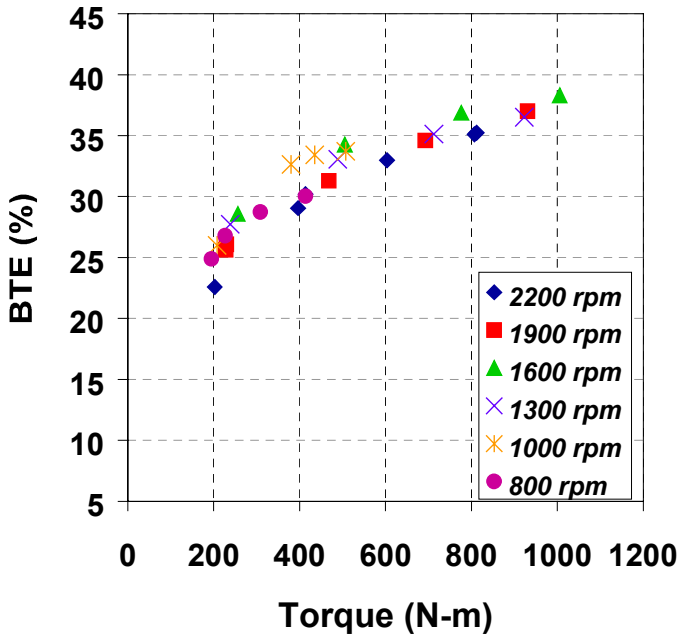

Figure 24. Brake Thermal Efficiency for FIPC Engine

Although these efficiencies are not equal to state-of-the-art natural gas engines, they are still relatively close to that obtained with some models of gas engines currently in use. Of more concern was the rapid drop off in efficiency as load was reduced below 300 lb-ft. Since this drop-off in efficiency occurred at all speeds, it was suspected that a reduction in combustion efficiency was the likely cause of the reduction in overall thermal efficiency.

This was confirmed by measurements of the unburned HC and carbon monoxide (CO) emissions. Figures 25 and 26 show the brake specific CO (BSCO) and HC (BSHC) emissions, respectively. Note that both BSCO and BSHC increase greatly as load is reduced. This was likely due to the increase in the percentage of fuel metered to the prechamber as load is reduced. At light loads, fuel was primarily concentrated in the prechamber due to its large size. In this situation, too much fuel was being burned in the prechamber, which contained rich zones that resulted in high hydrocarbon emissions. Another factor was, as load was reduced, the fraction of the fuel introduced to the prechamber was increased, and at some very low load conditions, only a small amount of fuel was entering the main chamber. For example, at the lowest loads shown, the prechamber fuel percentage was 70% while the prechamber volume was slightly less than 20% of the total combustion chamber volume. This high level of fueling in the prechamber corresponded to a very rich prechamber and a very lean main chamber. It is likely that this main chamber mixture was too lean to be ignited even by the prechamber jet, and this fuel was emitted as unburned hydrocarbons.

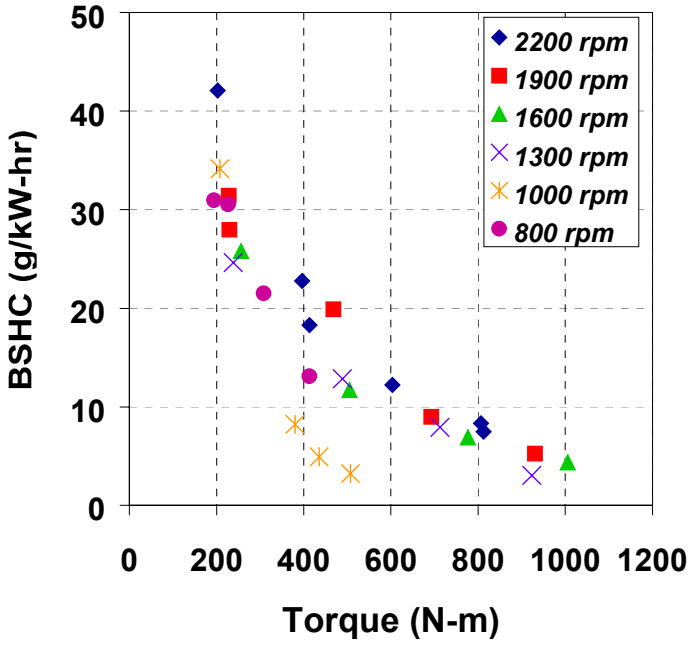

Figure 25. Brake Specific Hydrocarbon Emissions for FIPC Engine

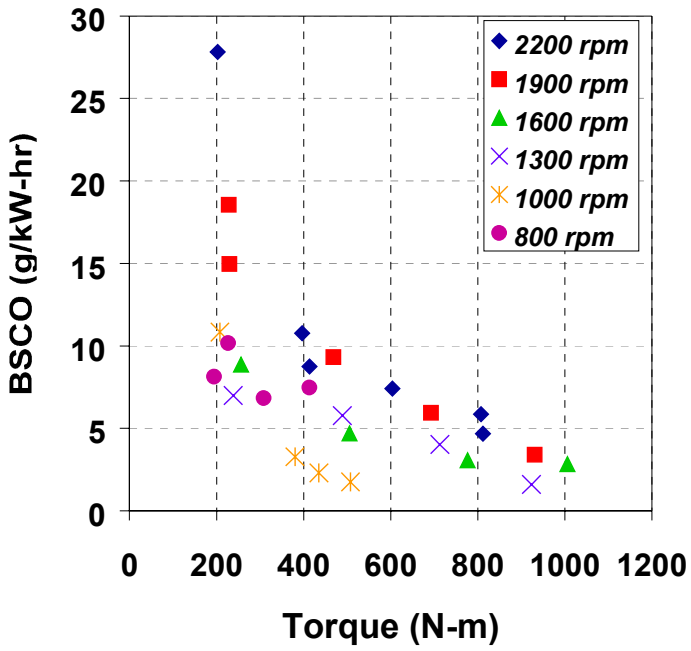

Figure 26. Brake Specific Carbon Monoxide Emissions for FIPC Engine

Rich mixtures produce high CO and increased HC levels compared to stoichiometric or lean mixtures due to insufficient oxygen for complete combustion. Also, very lean mixtures produce high HC and slightly increased CO emissions due to incomplete combustion at the lower temperatures encountered under these conditions. From an emissions point of view, the high CO and HC emissions are not an overriding concern, since an oxidation catalyst could be used to reduce their levels. An oxidation catalyst would be quite effective against CO, in particular. The high CO and HC levels are more of an efficiency concern, since they are indicative of an inefficient combustion process. Increased efficiency will be dependent on future improvements to combustion efficiency.

In addition, the high temperatures in the prechamber coupled with a high surface to volume ratio led to increased heat transfer losses. Also, it was noted that the oil sump temperature was much higher than normally seen on an open chamber engine. It was suspected that due to the large prechamber orifice used, the strength of the combustion jet caused a great deal of thermal energy to be deposited on the surface of the piston. This problem was confirmed by observation of hot spots on the piston at the point of jet impact.

NO_x emissions were also somewhat high as shown in Figure 27. For load points above 300 lb-ft, the NO_x emissions are relatively low, but NO_x did increase considerably for light loads at higher engine speeds. These high NO_x levels indicated that the prechambers were too large, since at light loads most of the fuel was burned in the prechamber so most of the NO_x is formed in the prechambers as well.

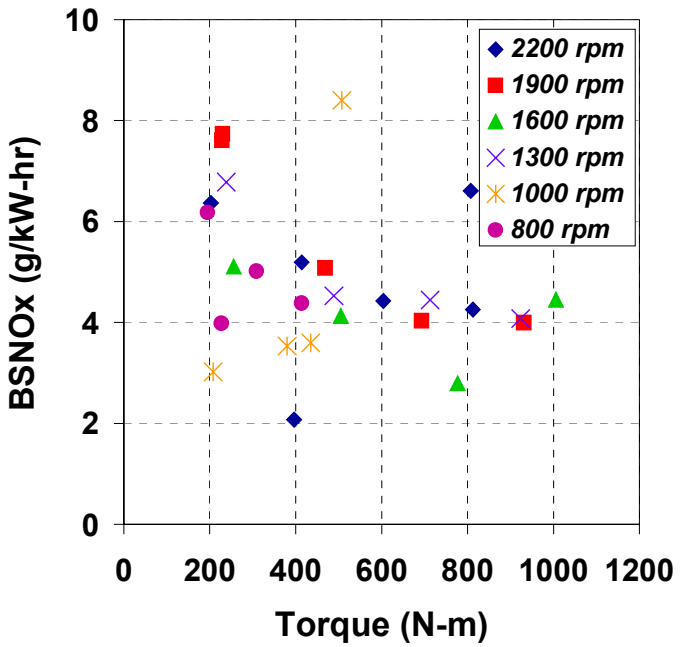

Figure 27. Brake Specific No_x Emissions for FIPC Engine

Following the emissions mapping exercise, some limited additional calibration work was conducted to investigate further reductions in emissions and increases in efficiency. At high loads, the prechamber fuel percentage was reduced. This appeared to help both emissions and efficiency and further confirmed that the prechambers were oversized.

6.0 Results with FIPC Engine with Reduced Volume Prechambers

To counteract these deficiencies, a smaller prechamber was designed. The prechamber size was reduced so that it contained less fuel at light loads, which forced more of the fuel to be burned in a premixed manner in the main chamber. The prechamber had to remain large enough to ignite the very lean mixtures expected at light loads, however. To investigate this, a prechamber with a volume equal to one-half that of the original prechamber was designed. The prechamber design equations yielded a design with the dimensions shown in Table 2.

Table 2. Revised Prechamber Specifications

Prechamber Parameter	Dimension
Volume	9.5 % (of clearance volume)
Nozzle diameter	6.0 mm
Craya-Curtet Number	0.278

A photograph of the revised prechamber is shown in Figure 28. The prechamber was designed as a self-contained insert that would fit in a slightly modified cylinder head. The hold down clamp was designed to be similar to those used on the original prechamber. Also shown is the prechamber as installed in the cylinder head. The hole towards the top of the prechamber is a spark plug hole, and the lower hole is the fuel introduction port. The fuel supply line is attached to this port.

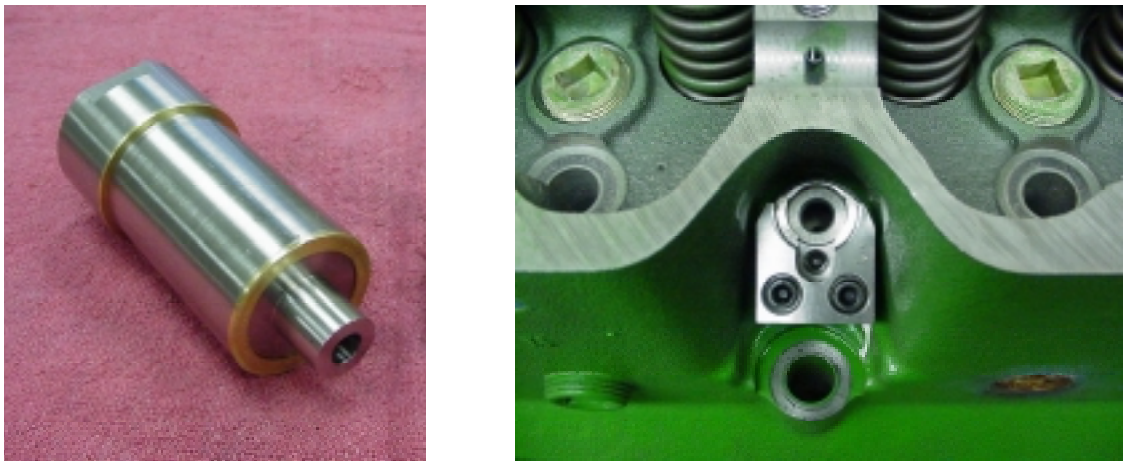

Figure 28. Reduced Volume Prechamber

The engine was equipped with a set of these prechambers. An extensive mapping exercise was conducted to optimize the calibration parameters. It was noted that the behavior of the engine changed markedly. For example, we found that the smaller prechamber was virtually insensitive to fuel injection timing over a broad range. Also, the problems encountered with oil and piston overheating were eliminated.

Test results obtained with the modified prechamber are shown in Figures 8-18. A plot of the engine's torque curve is shown in Figure 29. The project targets of 250 hp at 2200 rpm and 800

lb-ft at 1400 rpm were met. The low end of the torque curve was somewhat lower than desired due to the turbocharger match. The VNT 40 turbocharger has a turbine that is oversized for this engine, and at very lean conditions was unable to produce high levels of boost at low engine speeds without excessive back pressure on the engine. A smaller VNT was not available from Garrett for this project. At speeds above 1400 rpm, the turbocharger was able to provide adequate boost to meet the desired torque targets.

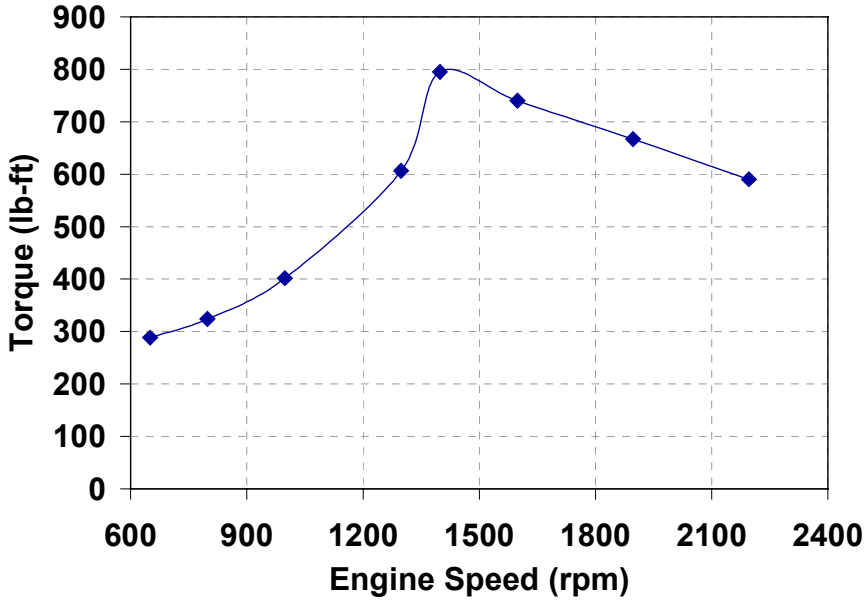

Figure 29. Torque Curve for FIPC Engine with Reduced Volume Prechambers

The torque characteristic of the engine is shown in Figure 30. Note that the engine operates much like a diesel engine, with a torque output that is very linear with respect to the torque command, i.e. the throttle input (or pedal position). This differs from a typical natural gas engine, which has a nonlinear throttle-torque relationship. A torque response that is linear with pedal position should provide good driveability in a vehicle application. The linear torque response is based on the linear increase in fuel flow rate versus pedal. Linear fueling and torque response is similar to that of a diesel engine, so this engine should provide a diesel-like “feel” to a driver.

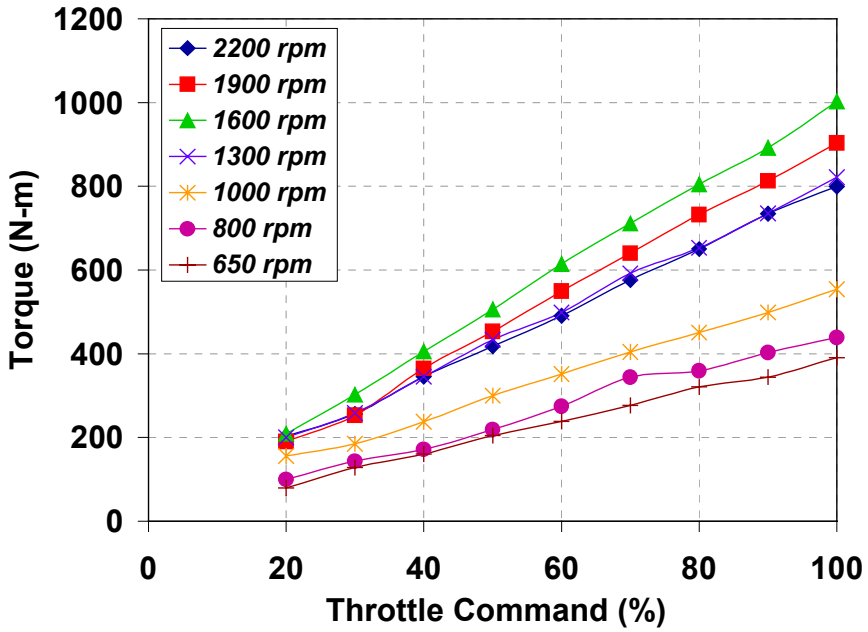

Figure 30. Torque Versus Throttle Characteristics for FIPC Engine with Reduced Volume Prechambers

Most notably, better performance was obtained when operating in the premixed "air mode" for nearly all conditions. Although the engine could operate at equivalence ratios below 0.5, optimum operation for best efficiency and emissions was found using a limited range of equivalence ratios. This narrower region of equivalence ratios can be seen in Figure 31. Over a wide range of load, the optimum equivalence ratio was approximately 0.55-0.60. This range is significantly leaner that of the lean misfire limit equivalence seen with typical spark ignited open chamber natural gas engines.

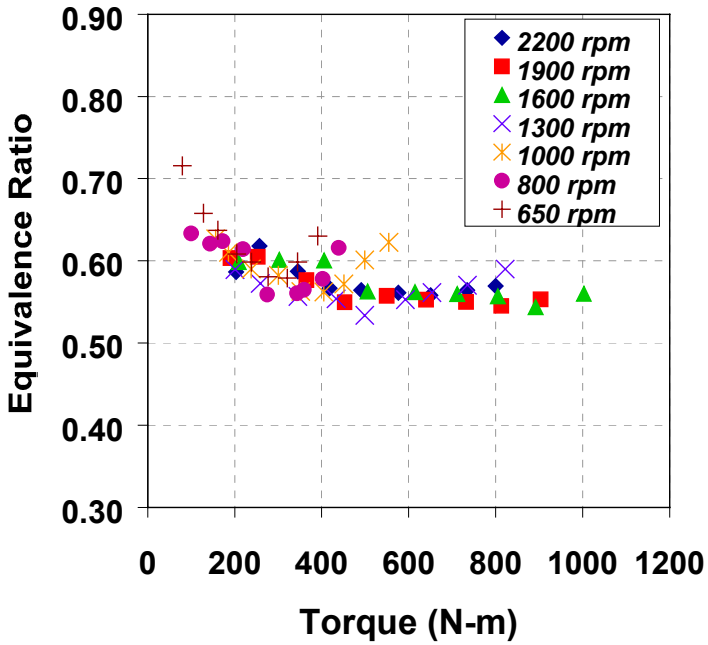

Figure 31. Equivalence Ratio Measured as a Function of Load for the FIPC Engine with Reduced Volume Prechambers

Since this range of equivalence ratio corresponds to an excessive amount of fuel flow for uninhibited air flow at light loads, some throttling was necessary. Figure 32 shows the extent of the throttling required at light loads.

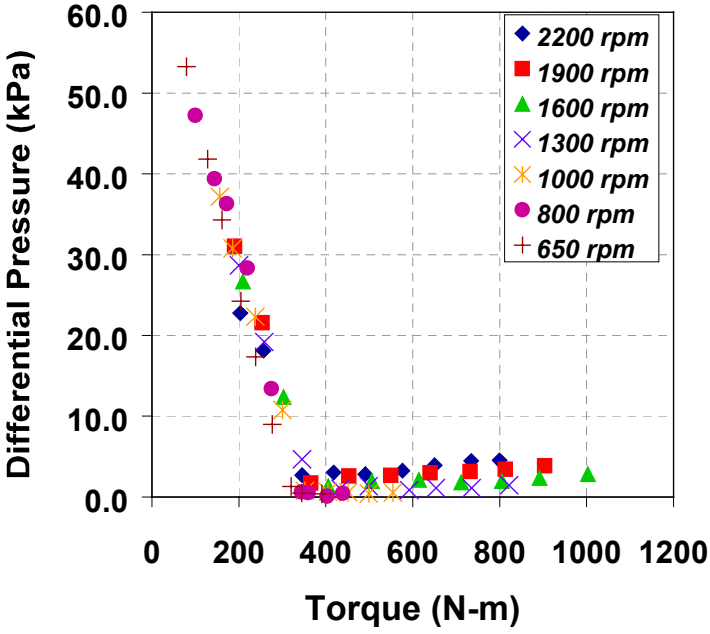

Figure 32. Pressure Drop Across Throttle Measured as a Function of Load for the FIPC Engine with Reduced Volume Prechambers.

Although the engine operated at very lean equivalence ratios well below those of the typical lean limit, the combustion stability was still good. Analysis of cylinder pressure data showed that for nearly all points, the coefficient of variation of the indicated mean effective pressure (COV_{imep}) was 2% or less. The COV_{IMEP} data is summarized in Figure 33.

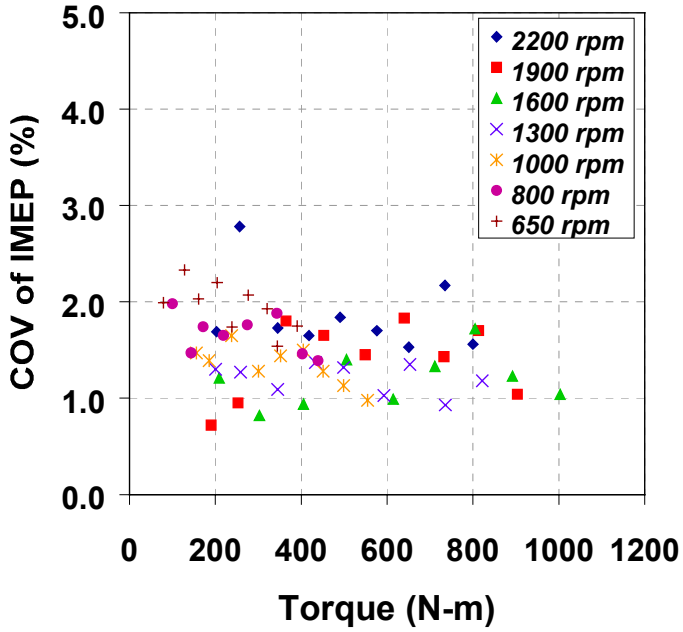

Figure 33. Combustion Stability for the FIPC Engine with Reduced Volume Prechambers

Along with good combustion stability, the engine also delivered high efficiency. The brake thermal efficiency as a function of load is shown in Figure 34. The maximum efficiency attained by the engine was over 40% at a speed of 1600 rpm. At the rated speed of 2200 rpm, the maximum efficiency was 38.3%. Both of these levels are quite competitive. An interesting feature of this plot is that the efficiency data appears nearly to fall along a single line.

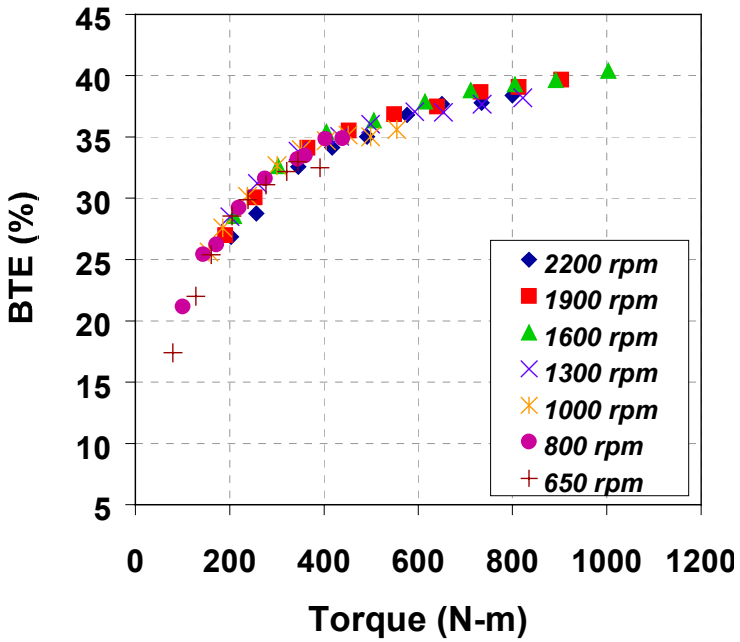

Figure 34. Brake Thermal Efficiency for the FIPC Engine with Reduced Volume Prechambers

The engine was also able to achieve NO_x emissions that were quite low. Figure 35 shows $BSNO_x$ emissions over the entire range of speeds and loads tested. Note that the $BSNO_x$ is primarily in the range of 1.0 to 2.5 g/kW-hr for all speeds and loads. It is also notable that the $BSNO_x$ levels at the highest efficiency points are below 2.0 g/kW-hr (1.5 g/bhp-hr).

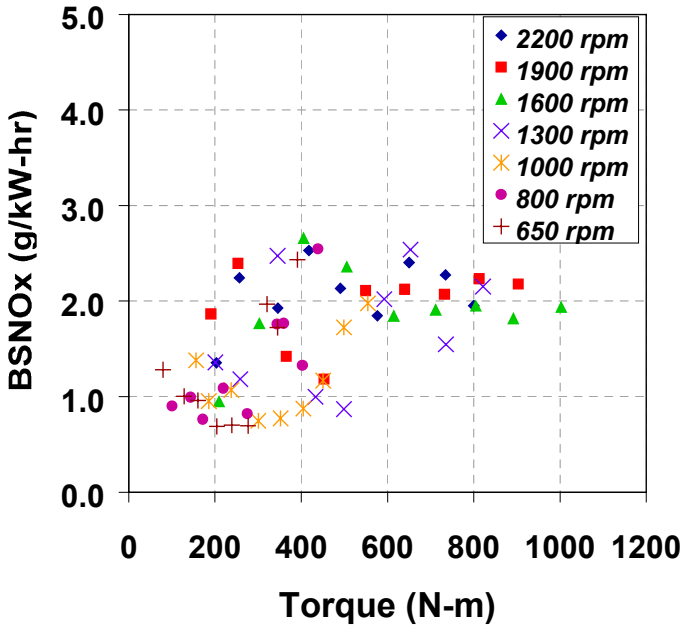

Figure 35. Brake Specific No_x Emissions for the FIPC Engine with Reduced Volume Prechambers

The ability of the FIPC engine to provide low NO_x simultaneously with high efficiency is shown directly in Figure 36, which is a plot of the $BSNO_x$ versus brake thermal efficiency tradeoff.

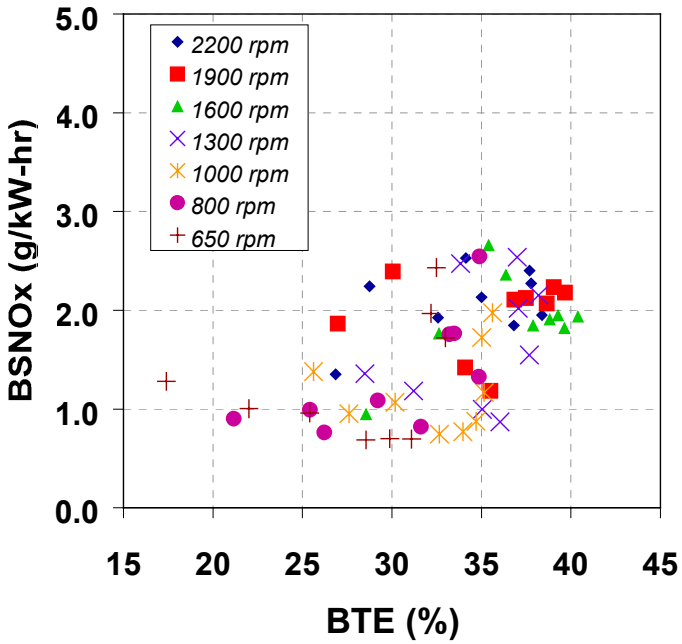

Figure 36. NO_x Versus Efficiency Tradeoff for the FIPC Engine with Reduced Volume Prechambers

Use of a smaller prechamber had the desired effect on fuel utilization and combustion efficiency. Figure 37 shows the significantly reduced HC emissions with the smaller prechamber. At low loads, BSHC ranged from 6-13 g/bhp-hr, roughly a 40%-60% reduction in BSHC compared to the large prechamber data.

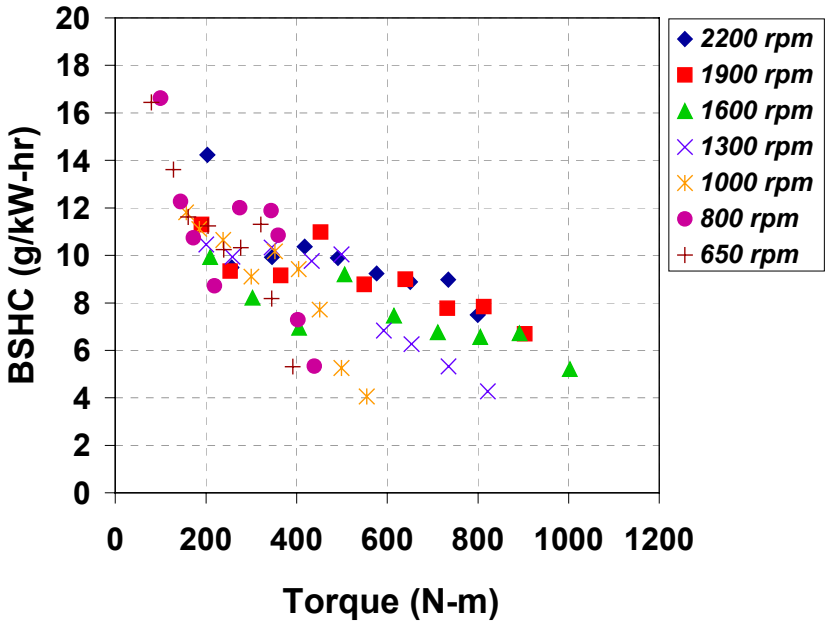

Figure 37. Brake Specific HC Emissions for the FIPC Engine with Reduced Volume Prechambers

Another indication that the fuel was being used more efficiently was the dramatic reduction in CO emissions. As shown in Figure 38, BSCO varied from 1-3 g/bhp-hr over the engine's operating range. These levels are comparable to the 1-2 g/bhp-hr levels seen with current on-highway CNG engines. Since the CO levels are in this range, it is likely that a substantial portion of the CO production is from incomplete combustion of the very lean main chamber mixture. Incomplete combustion of lean mixtures is the primary source of CO from typical homogeneous charge CNG engines.

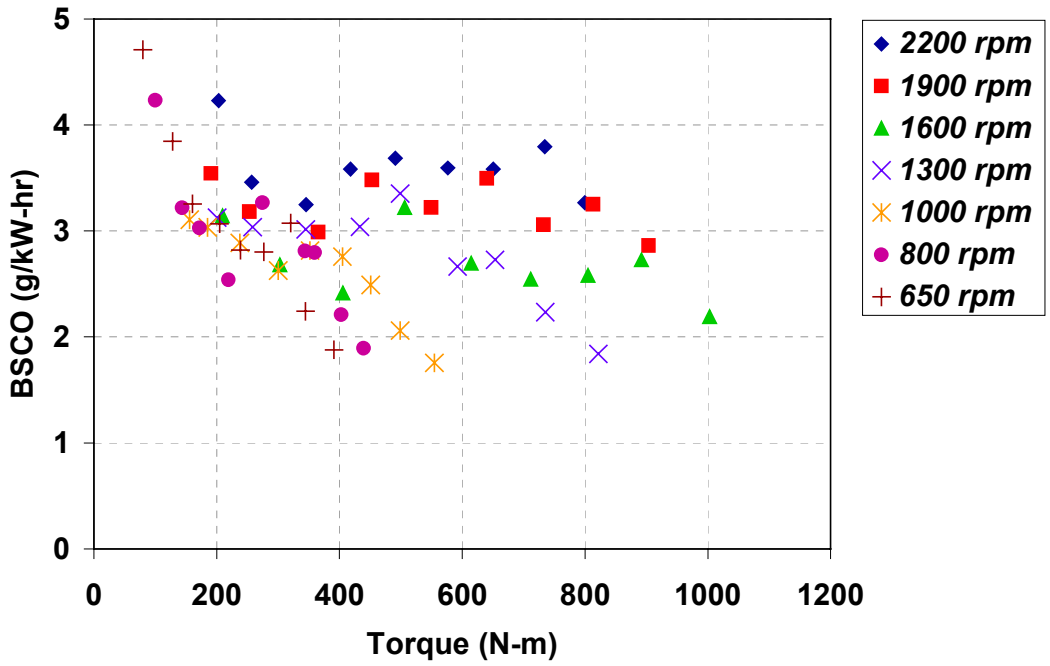

Figure 38. Brake Specific CO Emissions for the FIPC Engine with Reduced Volume Prechambers

6.1 Transient Emissions Estimation

Using the mapping data, the emissions from the engine over a U.S. EPA FTP transient test cycle were estimated. The SwRI FTP prediction method uses 12 steady state modes to predict engine emissions over an FTP test cycle. Table 3 shows the estimated results for the FIPC engine, in terms of brake specific NOx, nonmethane hydrocarbons (BSNMHC), CO, and brake specific particulate matter (BSPM). Note that particulate matter was not measured, and the BSPM number shown is an estimate based on the performance of current natural gas engines. The particulate emissions from the FIPC engine should be less than current engines due to the reduction in throttled operation, so less lubricating oil will be consumed and the resulting particulate emissions should be lower. Also included in the table is an estimate of the brake specific fuel consumption (BSFC) over the cycle.

Table 3. Estimated FTP Results from FIPC Engine

Pollutant	g/kW-hr	g/bhp-hr
BSNOx	1.64	1.22
BSNMHC	1.22	0.91
BSCO	3.26	2.43
BSPM	<0.025	<0.020
BSFC	240	180

A $BSNO_x$ level of 1.64 g/kW-hr (1.22 g/bhp-hr) is quite low, and very competitive with existing engines. The BSNMHC level of 1.22 g/kW-hr (0.91 g/bhp-hr) is somewhat high, but if an oxidation catalyst was used on the engine, this number could be reduced substantially. The BSFC shown is competitive with engines that are currently certified but is better than existing engines at this NO_x level.

7.0 Comparison to Existing Engines

Since the objective of the project was to develop an engine with enhanced efficiency compared to existing engines, the test data were compared to data from a similar 8.1L open chamber engine. The FIPC engine demonstrated some improvement in brake thermal efficiency compared to the open chamber (OC) engine. This improvement was prevalent over most of the load range of the engine. The following plot shows the brake thermal efficiency calculated for all speed-load combinations tested for both the FIPC and OC engines. Note that the FIPC advantage diminishes as load is reduced below 200 N-m, and the brake thermal efficiency for both engines dropped asymptotically to zero at idle.

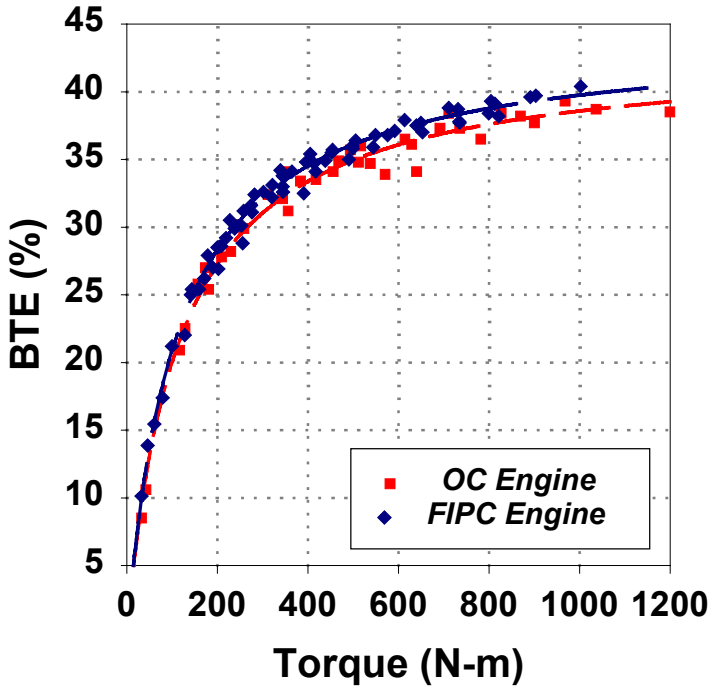

Figure 39. Brake Thermal Efficiency Comparison between the FIPC and Baseline Open Chamber Engine

Since the brake thermal efficiency approached zero at idle, it is more appropriate to compare the fuel consumption of two engines at idle conditions. Figure 40 shows the fuel consumption measured at the idle speed of 650 rpm at light load conditions. The brake mean effective pressure at this point was approximately 50 kPa. At these conditions, the FIPC engine provided a reduction in fuel consumption of approximately 17% as compared to the OC engine.

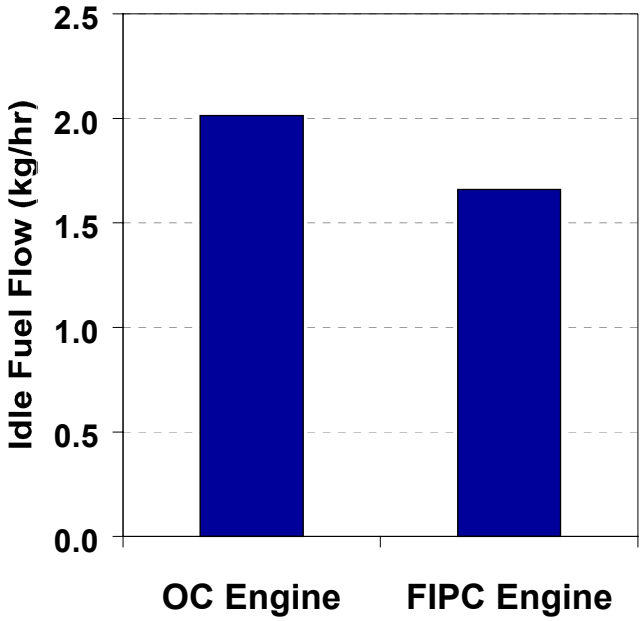

Figure 40. Idle Fuel Consumption Comparison between the FIPC and Baseline Open Chamber Engine

At high loads, the improvement in brake thermal efficiency could be attributed to the ability to run leaner with a higher combustion rate. At part loads, the improvement was due to the reduction in throttling. Although the FIPC engine required some throttling in its final configuration with the small prechambers, the amount of throttling losses remained small. A comparison of the throttling losses between the FIPC and OC engines is shown in Figure 41. This plot shows the pressure differential across the throttle as a function of load at 2200 rpm. Note the large reduction in pressure loss across the throttle with the FIPC engine.

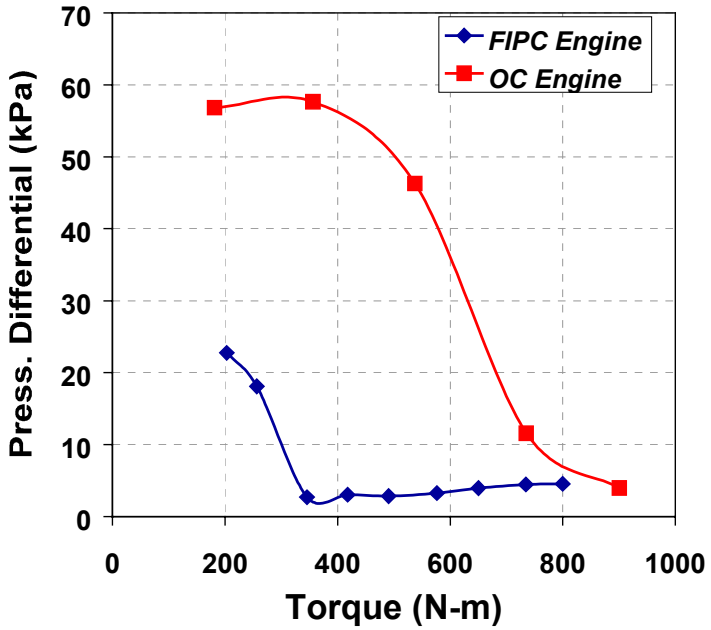

Figure 41. Comparison of Throttling Losses between the FIPC and Baseline Open Chamber Engine

One of the reasons that the increase in throttling losses did not affect brake thermal efficiency to a greater extent can be seen in Figure 42. This figure shows the reduction in combustion efficiency seen with the FIPC engine compared to an open chamber engine. Due to rich zones in the prechamber and ultra lean zones in the main chamber, the unburned hydrocarbon and CO emissions were higher than the open chamber engine. Since the combustion efficiency for the FIPC engine was lower, the overall brake thermal efficiency was accordingly lower.

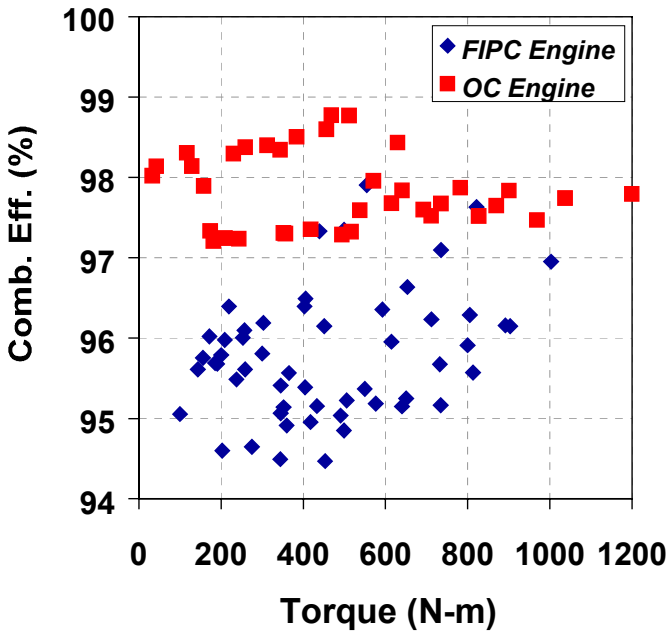

Figure 42. Combustion Efficiency Comparison between the FIPC and Baseline Open Chamber Engine

A fundamental way to compare the performance of two gas engine designs is to compare the tradeoff between NO_x emissions BTE for each engine. This has been illustrated in Figure 43. Note that the FIPC engine had a NO_x versus efficiency tradeoff that was somewhat better than the open chamber engine, particularly at high efficiency levels. This was primarily due to the FIPC engine running at considerable leaner equivalence ratios at these points.

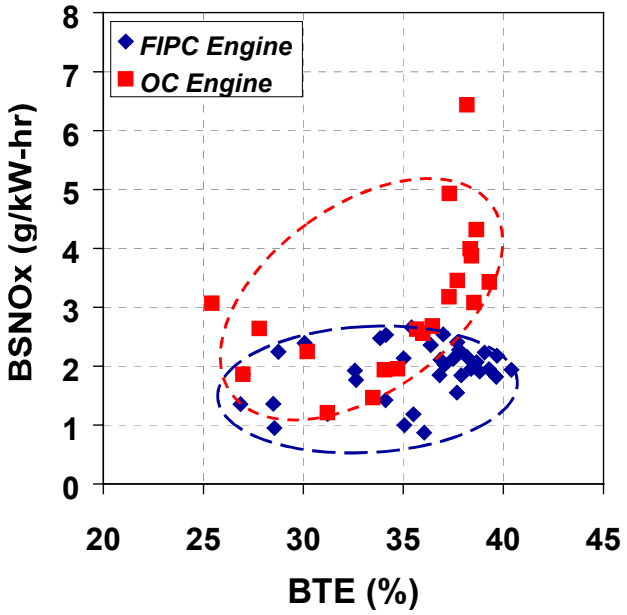

Figure 43. Comparison of the $BSNO_x$ versus BTE Tradeoffs for the FIPC Engine and the Baseline Open Chamber Engine

8.0 Conclusions

This project successfully demonstrated a novel lean burn engine combustion system aimed at a reducing part load fuel consumption while maintaining the emissions characteristics of current natural gas engines. Some of the specific findings from this project were:

1. Charge stratification through direct in-cylinder fuel injection was not feasible using the equipment available. The simple injector and combustion chamber design that was used was not capable of providing the level of fuel-air ratio control required for successful stratified charge operation.
2. Designing a successful direct natural gas injector is a complicated task that requires a great deal of effort to be devoted to it. In addition, extensive combustion development is required subsequent to a successful injector design.
3. Stratified charge operation that relies on spatial means to stratify the fuel-air mixture was found to be a more feasible method. In contrast to the DISC concept, the FIPC divided chamber engine concept worked well, and the engine could operate over the full speed and load range.
4. Existing prechamber design methods were found to work well in developing the FIPC engine. Also, simple automotive type port fuel injectors proved capable of providing precise control of fueling in the prechamber.
5. The FIPC concept engine provided good efficiency and combustion stability with low NO_x emissions. The NO_x versus efficiency tradeoff for the FIPC engine was improved compared to a state of the art natural gas engine. This increase was particularly significant at higher loads.
6. A significant reduction in fuel consumption at idle was also obtained with the FIPC engine compared to a state of the art natural gas engine. Fuel flow measurements at idle showed a reduction in fuel consumption of 17 percent with the FIPC engine.

In conclusion, the prototype FIPC engine demonstrated that part load and full load fuel economy improvements could be achieved on medium duty natural gas engines. The engine was able to satisfy the objectives of the project, i.e. obtaining these efficiency improvements while improving the emissions characteristics of the engine. As shown, the NO_x versus efficiency tradeoff for the FIPC engine was improved compared to a state of the art natural gas engine.

9.0 Recommendations for Future Work

Future development of this technology will pose some challenges. The current fuel system is complicated, and simplifying the FIPC fuel system would be an improvement. Simplification of the fuel system will be required to address concerns regarding manufacturing cost and overall system reliability. The initial cost of current natural gas engines tends to have a limiting effect on their adoption into mainstream use, so work will be required to reduce the number of fuel system components on the engine. This work will involve both design and development work. A cost-effective system will need to be designed, and subsequent testing will be required to confirm that this system can adequately maintain the performance and emissions aspects of the FIPC engine. Additional improvements in cooling and sealing the prechamber are also warranted. Since the prechamber and piston geometry used were quite simple, it is likely that continued optimization of these features would lead to further improvements in performance and emissions.

Using the FIPC concept may have additional opportunities as emissions regulations are pushed lower. In particular, it has been shown that the FIPC concept can provide a high energy ignition source for highly dilute fuel-air mixtures. Increasingly dilute mixtures will likely be encountered in the future, as engines are operated increasingly lean or with high levels of exhaust gas recirculation to reduce emissions.

References

1. NGV Part Load Efficiency Study, Gas Research Institute, Contract No. 5094-290-3010, September 1995.

2. Podnar D.J. and Kubesh, J.T., "Development of the Next Generation Medium-Duty Natural Gas Engine, Final Report," NREL/SR-540-27503, National Renewable Energy Laboratory, February 2000.

3. Alperstein, M., "Texaco's Stratified Charge Engine – Multifuel, Efficient, Clean, and Practical," SAE Technical Paper No. 740563, 1974.

4. Bishop, I.N. and Simko, A., "A New Concept of Stratified Charge Combustion – the Ford Combustion Process [FCP], SAE Technical Paper No. 680041, 1968.

5. Witzky, J.E and Hull, R.W., "The Development of the Pumpless Gas Engine Concept," SAE Technical Paper No. 700073, 1970.

6. Yagi, S., "NO_x Emission and Fuel Economy of the Honda CVCC Engine," SAE Technical Paper No. 741158, 1974.

7. Meyers, D.P., et al., "Evaluation of Six Natural Gas Combustion Systems for LNG Locomotive Applications, SAE Technical Paper No. 972967, 1997.

8. Quader, A.A., "The Axially-Stratified-Charge Engine, SAE Technical Paper No. 820131, 1982.

9. Callahan, T.J. and Kubesh, J.T., "Contribution of Prechamber Combustion to Engine CO and HC Emissions," Gas Machinery Conference, 1988.

10. Tatsuta, H., et al., "Mixture Formation and Combustion Performance in a New Direct-Injection SI V-6 Engine," SAE Technical Paper No. 981435, 1998.

11. Fraidl, G.K., "Gasoline Direct Injection: Actual Trends and Future Strategies for Injection and Combustion Systems," SAE Technical Paper No. 960465, 1996.

12. Kekedjian, A., and Krepec, T., "Further Development of Solenoid Operated Gas Injectors with Fast Opening and Closing," SAE Technical Paper No. 940450, 1994.

13. Gruden, D., et al., "Development of the Porsche SKS Engine," C243/76, Stratified Charge Engines, I Mech E Conference Publications 1976-11, November 1976.

14. Brandstetter, W.R., "Experimental Results from Volkswagen's Prechamber Stratified Charge Engines," C249/76, Stratified Charge Engines, I Mech E Conference Publications 1976-11, November 1976.

15. Ritter, T.E. and Wood, C.D, "An Unthrottled Gaseous Fuel Conversion of a 2-Stroke Diesel Engine," SAE Technical Paper No. 750159, 1975.

16. Anderson, A.C., et al., “The Development and Application of Design Criteria for Precombustion Chambers on Natural Gas Fueled Engines,” Technical Paper 84-DGP-1, American Society of Mechanical Engineers, 1984.

17. Kubesh, J.T., et al., “Lean Limit and Performance Improvements for a Heavy-Duty Natural Gas Engine,” SAE Technical Paper No. 961939, 1996.

REPORT DOCUMENTATION PAGE

Form Approved
OMB NO. 0704-0188

1. AGENCY USE ONLY (Leave blank)	2. REPORT DATE	3. REPORT TYPE AND DATES COVERED
	February 2002	Subcontract Report

4. TITLE AND SUBTITLE
Development of a Throttleless Natural Gas Engine

5. FUNDING NUMBERS
C: ZCI-9-29065-01
T: FU23.3310

6. AUTHOR(S)
John Kubesh

7. PERFORMING ORGANIZATION NAME(S) AND ADDRESS(ES)
Southwest Research Institute
6220 Culebra Road
San Antonio, TX 78238-6166

8. PERFORMING ORGANIZATION REPORT NUMBER

9. SPONSORING/MONITORING AGENCY NAME(S) AND ADDRESS(ES)
National Renewable Energy Laboratory
1617 Cole Blvd.
Golden, CO 80401-3393

10. SPONSORING/MONITORING AGENCY REPORT NUMBER
NREL/SR-540-31141

11. SUPPLEMENTARY NOTES
NREL Technical Monitor: Mike Frailey

12a. DISTRIBUTION/AVAILABILITY STATEMENT
National Technical Information Service
U.S. Department of Commerce
5285 Port Royal Road
Springfield, VA 22161

12b. DISTRIBUTION CODE

13. ABSTRACT *(Maximum 200 words)*
Subcontract report describing a project to investigate methods to increase the efficiency of natural gas engines, especially under part-load conditions. Report contains details on the development of a natural gas-fueled engine capable of throttleless operation to improve part load efficiency.

14. SUBJECT TERMS
throttleless; natural gas; part-load; FIPC

15. NUMBER OF PAGES

16. PRICE CODE

17. SECURITY CLASSIFICATION OF REPORT	18. SECURITY CLASSIFICATION OF THIS PAGE	19. SECURITY CLASSIFICATION OF ABSTRACT	20. LIMITATION OF ABSTRACT
Unclassified	Unclassified	Unclassified	UL